Lung (2002) 179:333–373
DOI: 10.1007/s004080000073

Lung
© Springer-Verlag
New York Inc. 2002

Airway Smooth Muscle

N. L. Stephens

Department of Physiology, Faculty of Medicine, University of Manitoba, Basic Medical Sciences Building, 730 William Avenue, Winnipeg, MB Canada R3E 3J7

Abstract. The greatest impetus to research in elucidating the fundamental biophysics and biochemistry of airway smooth muscle (ASM) has undoubtedly been provided by the need to understand how these are altered in asthma. Many of the biophysical and biochemical properties of this muscle have been reviewed before (Stephens, 1970; Stephens, 1977; Mulvaney, 1979; Souhrada and Loader, 1979; Stephens and Kroeger, 1980). They resemble those of striated muscle; however, even though mechanical properties are very similar, there are differences in biochemistry. For example, in smooth muscle, calcium-sensitive regulation of contraction is mediated by a calmodulin/myosin-light-chain kinase/phosphatase system, not by the familiar troponin-tropomyosin system (Gorecka et al., 1974; Mrwa and Ruegg, 1975; Dillon et al., 1981; Aksoy et al., 1982). Thus, the molecular mechanisms to be investigated in understanding disorders of increased smooth muscle contraction, which occur in allergic bronchospasm (Souhrada and Dickey, 1976), for example, may be quite different from those in striated muscle. Much of the following material is based on studies of canine tracheal smooth muscle (TSM) because there is evidence (Jenne et al., 1975) that it serves as a model for ASM—at least with respect to contractility down to the sixth generation of airways. Studies of isolated smooth muscle from smaller airways (Russell, 1978) are few and are based mainly on studies of lung strips (Lulich et al., 1976). Since then, we have developed a bronchial smooth muscle preparation (fifth generation) that allows precise study of those airways that are involved in allergic bronchospasm. Considerable work has been carried out on ASM from a variety of animal models of asthma. It should be pointed out that none of these reproduces the human disease exactly, and that they really should be identified as examples of nonspecific hyperreactivity. Be that as it may, the nonspecificity found in human patients *in vivo* and in animals (Peterson et al., 1971; Hargreave et al.,

Correspondence to: N. L. Stephens; E-mail: nstephe@ms.umanitoba.ca

1980) suggests that the primary cause of asthma may reside at the muscle cell level. Whether it is the cell membrane, the excitation–contraction coupling apparatus, or the contractile machinery that is primarily involved, is not yet known with certainty.

Key words: Airway smooth muscle—Asthma—Tracheal smooth muscle

Structure of Airway Smooth Muscle

In all mammalian species the tracheal smooth muscle is found dorsally, bridging the ends of the incomplete C-shaped cartilaginous rings of the trachea. These rings are also C-shaped in the main bronchi, but this feature becomes modified lower down where discrete cartilaginous plaques are found. In bronchoconstriction, as the airways narrow, these plaques approach each other and imbricate, thus providing stability and protection from collapse; Vanpeperstraete (1973) has reported that there is considerable variability in the cartilaginous skeleton. Avian cartilage completely surrounds the trachea and main bronchi, and there is no membranous portion. In the dog the ends of the *C* almost touch each other dorsally, leaving only a small gap bridged by a small fibromuscular membrane.

The posterior or dorsal membrane is really made up of two membranes, with one of muscle and the other of epithelial and connective tissue. Considerable variation exists in the relationship between these two structures. Even though the muscle layer is ventral to the connective tissue layer in the human, guinea pig, and hedgehog, it is dorsally apposed in the dog, cat, and rabbit.

The muscle layer or *musculus transversus tracheae* consists of a unified layer of thick bundles of smooth muscle characterized by minimal branching and transverse orientation. The bundles are attached by tendons to the external perichondrium (near the dorsal ends of the cartilage) and the annular ligaments. In humans the insertion is on the internal perichondrium. Slips of muscle also insert into the ventral esophagus. The vascular supply to tracheobronchial smooth muscle is derived from the bronchial artery. Perhaps some oxygen is obtained directly by diffusion from gas in the lumen.

The trachea and the distal airways arise from the foregut and share some of the morphological characteristics of the gastrointestinal tract. It is not surprising, therefore, to find very similar neural control.

With respect to growth, the quantity of airway smooth muscle increases as the child grows; however, the number of mucous gland decreases. In studies of fetuses (Hakansson et al., 1976) the circumferential muscles were found in an inner and an outer layer; the former were circular and the latter were longitudinal and organized into bundles,. A muscularis mucosa was present beneath the tracheal mucosa and resembled that of the intestine. Although the longitudinal muscles were clearly seen in the newborn and in infants, they disappeared with adulthood.

Small Bronchi

Little investigation of the musculature of the small airways (those with a diameter less than 3 mm in humans) has been carried out. Daniel et al. (1986) reported that musculature of the first- and second-generation human bronchi showed almost the same characteristics as those of the trachea; however, those from the fourth to the seventh showed differences. The muscle bundles were small and the cells were irregularly orientated. The number and size of gap junctions were much smaller than were those of the trachea. The contractile filaments also revealed variability. Some thick filaments were ribbonlike. Mast cells seemed to bear a closer relationship to bronchial smooth muscle than to tracheal.

With regard to innervation, these workers found a much denser innervation in the smaller bronchi than in the trachea. They concluded that tracheal smooth muscle is organized for myogenic control with secondary neural modulation, whereas bronchial smooth muscle is organized for neural control.

To return back to the trachea for a moment, another important observation of Daniel et al. (1986) is that gap junctions can form within minutes *in vitro* in human tracheal smooth muscle.

Single Unit, Multiunit, and Intermediate Types of Smooth Muscle Cell

Burnstock (1979) has classified smooth muscle into three types. Single unit cells are seen in tissues such as the intestinal tract, taenia coli, ureter, resistance arteries, and arterioles and uterus at term. Such tissues show spontaneous, rhythmic contractions and also develop trains of action potentials. The resting membrane potential is not as stable as it is in multiunit smooth muscles, but displays oscillations. Action potentials generally, although not always, arise from the peaks of waves. Single unit muscle possesses a strong myogenic response. The smooth muscle cells show a large number of cell-to-cell communications (so-called gap junctions) that are of low impedance and facilitate propagation of the action potential. There is a paucity of nerves, and those that exist function to modulate the spontaneous myogenic activity. This combination of paucity of nerves and large numbers of intercellular gap junctions is typical of single unit smooth muscle cells. Multiunit smooth muscle cells are so termed because each cell is separately innervated. Innervation is accordingly dense, and low-impedance gap junctions are few. Such muscles show no spontaneous rhythmic activity and no myogenic response. Action potentials are usually absent and the response to agonists is via graded depolarization of the membrane. The membrane at rest is more polarized than that of single unit smooth muscle cells. Pacemaker cells, so typical of single unit cells, are not seen in multiunit cells. Examples of multiunit smooth muscle cells are those present in the larger and medium-sized blood vessels and the larger bronchi.

The canine tracheal smooth muscle falls into an intermediate category because even though gap junctions are few, innervation is not very dense.

Considerable interest has been aroused by the fact that multiunit smooth muscle can be converted into single unit type. Kroeger and Stephens (1975),

Suzuki et al. (1976) and Daniel et al. (1986) have shown that tetraethylammonium salts and 4-aminopyridine can effect this change. Daniel's group has shown that the change is associated with rapid induction of gap junctions, which is not blocked by inhibitors of protein synthesis, and conclude that the junctions result from assembly of preformed proteins.

It has been suggested by Macklem (personal communication) that allergic or asthmatic bronchospasm could result from the conversion of multiunit airway smooth muscle to single unit type. This could certainly account for the increased excitability of asthmatic airways, but whether it also accounts for the increased narrowing—the hallmark of asthma—has yet to be established.

Structure of Airway Smooth Muscle Cells

The canine TSM cell is long and narrow, measuring 1000 μm by 5 μm, according to Suzuki et al. (1976). Kroeger and Stephens (1971) have found that on average it is about 250 μm long and 3–5 μm wide at the level of the nucleus.

Lower power electronmicrographs (Fig. 1) reveal that the cells are arranged in bundles separated by fairly wide and variable interfascicular spaces. These spaces contain collagen, elastin (in both amorphous and fibrillar form), fibroblasts, neural axons, blood vessels, and mast cells. Analysis has shown that on average, a bundle contains about 300–400 cells. Approximately 10% of the cells per bundle—entirely on the periphery and in the interfascicular space—are fibroblasts. Though extremely long and tortuous, their volume is very small and they represent less than 5% of the volume of the bundle.

The smooth muscle cells in the adult canine TSM represent 75% of the tissue. This feature renders it a suitable preparation for both biophysical and biochemical studies. For Fig. 1, the muscle strip was fixed during maximal isometric contraction at optimal length (l_o). Measurements of the muscle's series elastic component (Stephens and Kroeger, 1975; Stephens and Hoppins, 1980) indicate that the maximal internal shortening of the cell in an isometric contraction is about 7% of l_o. The fact that the cells maintain parallel orientation, even at peak contraction, is noteworthy because longitudinal forces will continue to be transmitted effectively to the ends of the muscle.

Figure 2 shows an electronmicrograph of muscle fixed at l_o, but in a completely relaxed state. The parallel orientation of the cells is clear. It must be pointed out that parallel alignment of the cells is not a sufficient condition for mechanical efficiency in itself. The important factor is the orientation of the contractile filaments within the cell. Bagby (1971) has indicated that in the toad stomach muscle these filaments traverse the cell obliquely; however, Gabella (1976) believes they run parallel to the longitudinal cellular axis in the taenia coli. In the canine trachealis (Fig. 1) the cell outlines are crenated, suggesting oblique orientation of the filaments within the cells; nevertheless, where filaments (e.g., at the cell periphery) are clearly seen they seem to run in the longitudinal axis. From a functional point of view the maximum force developed by a muscle will be recorded when the force-measuring device is orientated

Fig. 1. Montage of a single bundle of isometrically contracted canine tracheal smooth muscle cells were constructed from low-power electron micrographs. The perifascicular space above the muscle cells contains collagen, a vessel, several fibroblasts, and a mast cell with dark granule. Light and dark cells are seen. The cell outlines of the light cells suggest they are swollen. The crenate outlines of the dark cells and the twisted shape of the centrally placed nuclei indicate the cells are contracted. The thick rectangular, vertical calibration bar represents a length of 10 μm (mag × 4000).

Fig. 2. Electronmicrograph of a longitudinal section of canine tracheal smooth muscle. A = Actin filaments; BM = basement membrane; Mit = mitochondria (these are long and serpiginous); CF = collagen fibriels; PV = pinocytotic vesicles; MS = myelin swirls; DB = dense bodies (mag × 16,500). (Source: From Nadel, JA Physiol and Pharmacol of the Airways, Marcel Dekker, New York, 1980, with permission.)

in the same axis as the force-generating filaments. This may be determined by cutting muscle strips from the tracheal muscular membrane at a variety of helical angles and noting in which strip maximum isometric force (P_o) develops. This is seen in the trachealis in the strip whose longitudinal axis coincides with the long axis of the cells. This proves that in this muscle, contractile filaments are not obliquely oriented. All the muscle cells in the trachealis run transversely, bridging the ends of the cartilaginous rings.

As stated earlier, Fig. 1 shows that the space between the bundles contains blood vessels, two of which are seen in the upper left-hand corner. Most of the cells in the space, in Fig. 1, are fibroblasts. A single mast cell, which is characterized by its granules, is also seen.

Nerve filaments run in the interfascicular space apparently toward the muscle cells. They will be discussed later. It must be recognized at this point that, even though innervation of the outermost layer of cells in the bundles seen, hardly any nerve terminals are seen innervating the cells in the core of the bundle. The question then arises as to how these cells are stimulated. One possibility is that the central cells are of the single-unit variety and are activated by cell–cell transmission from the outer cells, which are of multiunit or intermediate type. No careful study of the problem has yet been carried out. If the central cells *are* of the more excitable, single-unit type, we should expect to see many gap junctions (i.e., low impedance, electron-dense areas of contact between cells) on their sarcolemmas. Our preliminary studies have not demonstrated this. The other speculation is that as the central cells are not innervated, they may possess the type of supersensitivity seen in denervated muscle cells. Because of this they could be induced to contract even though the depolarizing current reaching them is weak.

Specialized Features—Cell Membrane or Sarcolemma, Pinocytotic Vesicles, and Basement Membrane

In Fig. 2, the sarcolemmal membrane of smooth muscle cells is clearly visible. High-power micrographs have confirmed that the sarcolemma in TSM is similar in structure to that of other types of muscle and nonmuscle cells in possessing a lipid bilayer with protein elements traversing it. Figure 3 is a higher-power micrograph of a longitudinal section of tracheal smooth muscle fixed in isotonic contraction. The typical crenation of the membrane is present. The tissue had undergone considerable shortening such that the sarcolemma developed sizeable outpouchings. Fay (1977) has shown that the entire surface is covered with similar outpouchings in isolated single cells, where considerably more shortening occurs. The pouches contain organelles such as pinocytotic vesicles and sarcoplasmic reticulum, but no contractile filaments. The cell at the bottom of Figure 3 shows this quite clearly. It also shows that the contractile filaments (the majority are thin filaments) run parallel to the long axis of the cell and do not enter into the outpouchings.

Figures 2 and 3 show a large number of vesicles—the pinocytotic vesicles (PV). The majority appear as complete vesicles and lie under the sarcolemma. Some open onto the sarcolemmal surface and are incomplete. They appear to be filled with basement membranelike material. The vesicular membranes show the same structure as the sarcolemma. The function of these vesicles is not clear, but they considerably increase the total surface area of the cell. This would facilitate exchange of fluid, nutrients, and ions across the membrane. Gabella (1976) has reported that in most smooth muscle cells caveolae or micropinocytes are flask-shaped, and are about 70 μm across and 120 nm in length. He reports a ring of intramembrane particles around their openings, and it is possible that they are specific for smooth muscle cells. In the taenia coli there are 30–35 caveolae/μm^2 of membrane, or about 170,000 per cell. No similar quantitative studies have been carried out for airway smooth muscle. The membranes in the taenia show

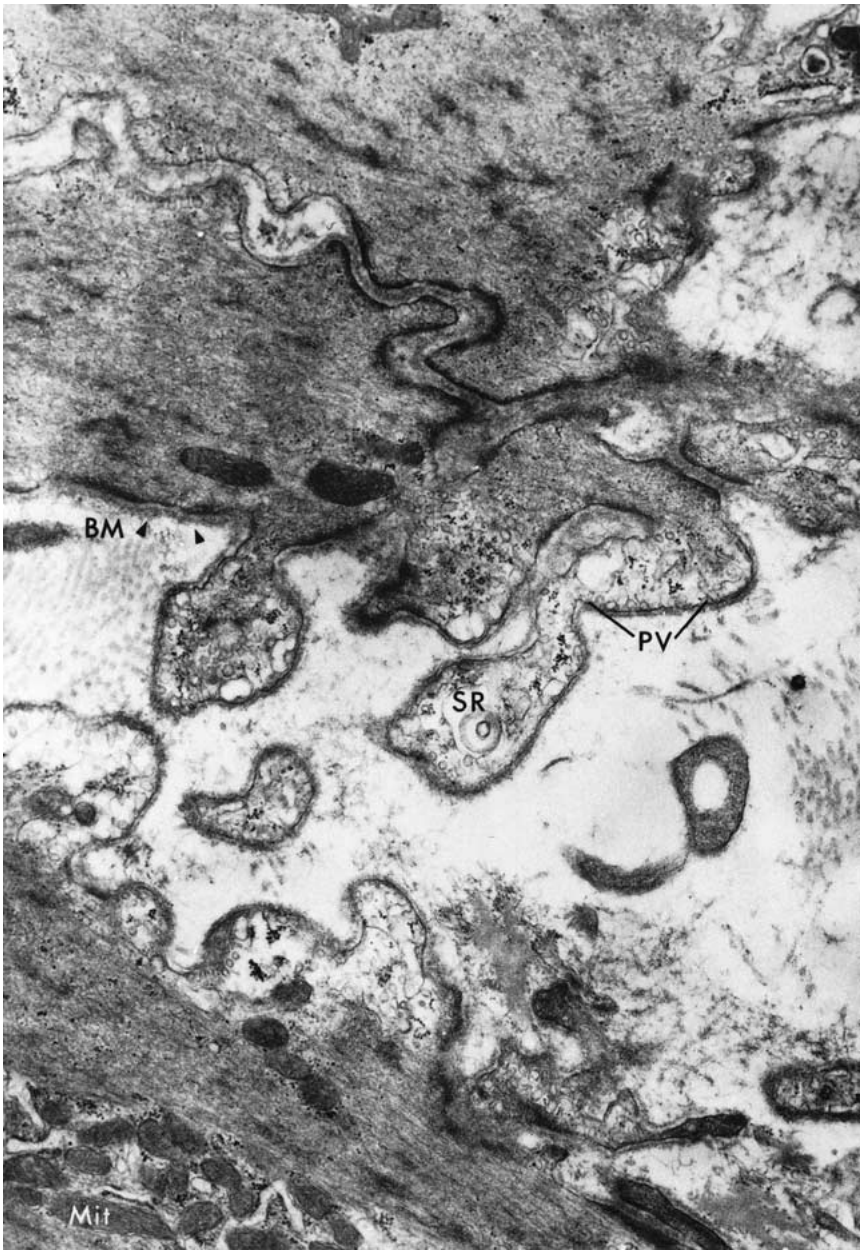

Fig. 3. Electronmicrograph (mag × 26,000) of longitudinal sections of canine tracheal smooth muscle. BM = basement membrane with a group of fibrillar elements close to it. External to the fibrils is a bundle of collagen fibers, some of which are cut transversely and others tangentially. This suggests that they wind around muscle cell bundles. SR = sarcoplasmic reticulum (swollen); Mit = mitochondria in orthodox state. The first and second cells from the top are in fairly close apposition. Much of this zone shows electron-dense patches in the sarcolemma—these are termed *dense bands*—with condensation of intercellular material forming an intermediate junction. Several sarcolemmal out-pouchings are seen, which indicates the muscle is isotonically shortened.

Ca^{2+}-ATPase activity, so they are probably involved in regulating calcium fluxes. In addition, they are said to control Na^{+} and water flow across the cell membrane. In some areas the pinocytotic vesicles, sarcoplasmic reticulum, and sarcolemma (and occasionally mitochondria) are in close contact. This may form a type of excitation–contraction coupling apparatus. T-Tubules, of course, are not seen in smooth muscle cells. This fact is not a serious disadvantage; because the cell diameter is extremely small, hence propagation of electrical activity from the sarcolemma to the innermost contractile units is not a problem.

The surface–volume ratio in airway smooth muscle is high, which is in common with other smooth muscle cells. This ratio varies from tissue to tissue (1.5 in taenia coli of guinea pig and 2.7 in the sphincter pupillae according to Gabella (1976); unfortunately, no quantitative studies have been undertaken in airway smooth muscle.

The basement membrane (BM) is clearly seen in Figure 3. It surrounds the cell and shows increased electron density where it overlies specialized areas of the sarcolemma, known as *dense bands*. A clear separation is seen between the basement membrane and the sarcolemma. The basement membrane is about 25 nm thick. It extends over caveolae and dense bands and penetrates into intermediate junctions. It may be seen entering the space between nerve ending and muscle cell surface; it is not seen in gap junctions. Collagen fibrils appear to run into the basement membrane, as do fibrillar elastic elements.

Sarcoplasmic reticulum (SR) exists in rudimentary form in airway smooth muscle. Figure 3 shows a dilated example. It normally exists as a tubular structure but does not show the organization of the SR of striated muscle. Where no organized excitation–contraction coupling apparatus is seen in smooth muscle, the occasional contiguity of SR, sarcolemma, pinocytotic vesicle, and mitochondria hints at the rudiments of such an apparatus, as suggested earlier.

Microsomal preparations obtained from SR elements (as distinct from sarcolemmal) have been described that possess Ca^{2+}-ATPase activity and bind and take up calcium.

Dense Bands, Dense Bodies

Much interest has been aroused by these structures because it has been realized that they are likely analogues of the Z discs of striated muscle. They could thus delineate sarcomeres in smooth muscle. These ideas are new and exciting because it was precisely the absence of sarcomeres, along with failure to demonstrate thick filaments, that led to the muscle being termed *smooth*.

Dense bands are areas of increased electron density in segments of the sarcolemma. Typical examples are seen in Figure 3, especially in the region where cells come close together. They are fewest in the part of the sarcolemma overlying the nucleus and increase in number toward the periphery of the cell. The membrane overlying the ends of the cell is almost completely electron-dense. Similar dense structures are found scattered throughout the cytoplasm. In this location they are called *dense bodies* (db).

Dense bands are formed by a layer of electron-dense material adhering to the cytoplasmic side of the cell membrane. As pointed out by Gabella (1976), they are more prominent in contracted muscle than they are in relaxed muscle. The relatively recently recognized intermediate filaments appear to run into the dense bands, especially at the cell ends. α-actinin appears to be localized specifically in dense bands and dense bodies, where it has been studied with the help of antibody techniques by Fay (1997) and Somlyo (1980). Metavinculin, a 130,000-dalton molecular weight protein, has also been found in, but is not confined exclusively to, the dense bands.

Even though it is likely that these proteins are also present in AMS, no specific studies have yet been conducted.

Visceral muscle dense bands are about 0.2–0.4 μm wide and up to 2 μm long. In tracheal smooth muscle we have found that the length of the dense bands is 0.4 ± 0.01 μm (SE). Intermediate junctions form where dense band areas of the sarcolemma of two cells come in close apposition. The average length of the intermediate junction is 0.26 ± 0.01 μm (SE). Measurements also show that these junctions contribute 70% of the dense band area.

Gabella has suggested that the intermediate junctions serve to transmit mechanical forces laterally or obliquely between cells. Because of the insertion of actin filaments on the cytoplasmic aspect of the dense bands, he also thinks that dense bands provide mechanical coupling between the myofilaments and connective tissue stroma. In these areas the basement membrane is specially thickened and receives insertions from microfibrils.

Contrary to the belief that smooth muscle cells are fusiform in shape, we find in tracheal smooth muscle, as has Gabella in the taenia coli, that the end of the cell splays out into a convoluted footlike process. The foot processes from adjacent cells appear to be linked together by condensations of the stroma. These end-to-end intermediate-type junctional connections serve to transmit mechanical forces along the longitudinal axis.

Gap Junctions

The importance of these junctions lies in the consideration that these are areas of low electrical impedance and serve to transmit a wave of depolarization from cell to cell, thereby producing a functional syncytium. In gap junctions the intercellular gap is only 2–3 nm wide. Figure 4 shows a gap junction in tracheal smooth muscle. Because the muscle cells and larger airways are of the intermediate type described by Burnstock (1979), we did not expect to find many gap junctions, and such indeed turns out to be the case. Daniel et al. (1986) reported that their frequency is 2.7 ± 0.3 (SE) per 100 smooth muscle cells.

Multiunit smooth muscle, as stated before, is generally not spontaneously contractile, does not manifest action potentials, and is devoid of a myogenic reflex. Several investigators (Kroeger and Stephens, 1975; Suzuki et al., 1976) have shown that when it is treated with tetraethylammonium or 4-aminopyridine, the muscle develops typical single unit characteristics: spontaneous rhythmic ac-

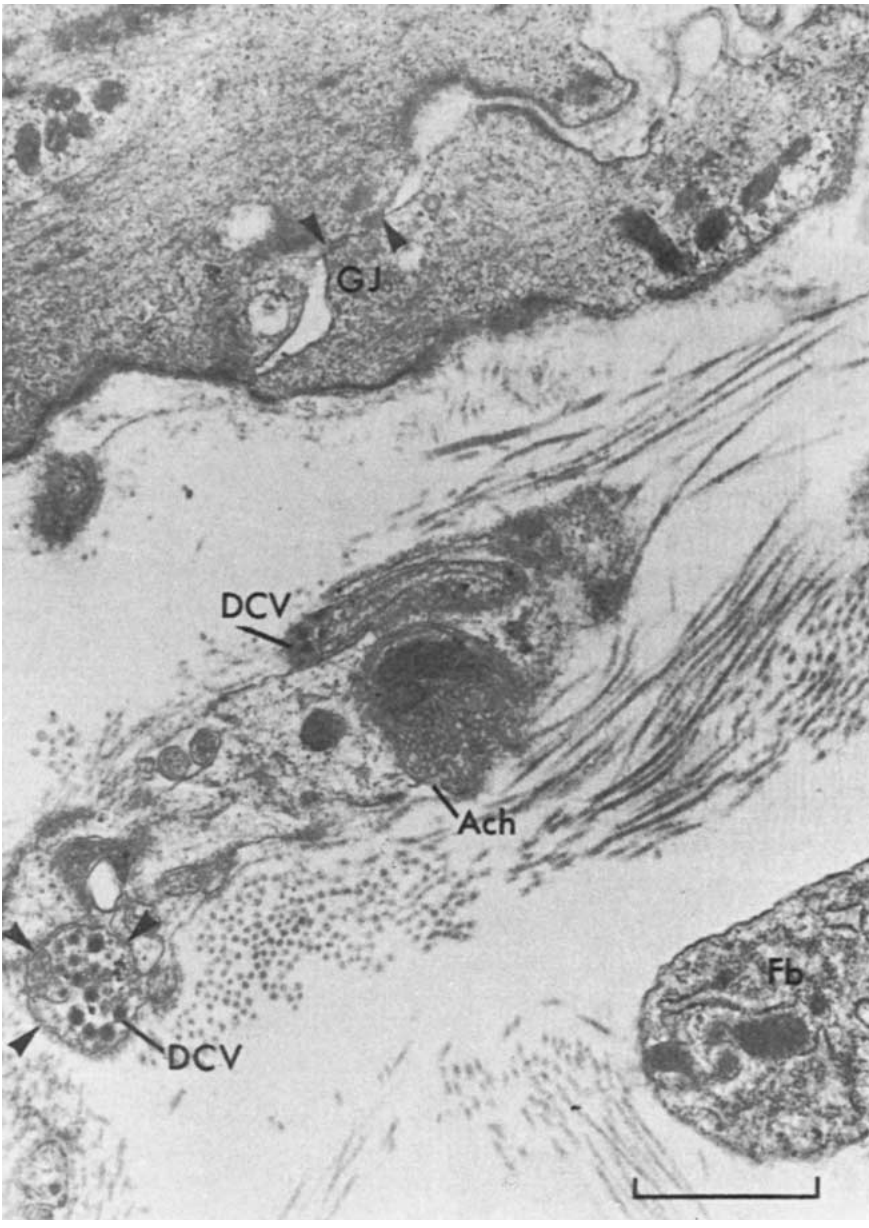

Fig. 4. Electronmicrograph of longitudinal sections of canine tracheal smooth muscle, (mag × 26,000). GJ = gap junction; DCV = dense cored vesicle; ACh = small clear vesicles containing acetylcholine; Fb = fibroblast.

tivity, action potentials, and a myogenic response. Daniel's group has shown that a large number of gap junctions also develop in such preparations. These could subserve cell-to-cell electrical transmission. The junctions appear to be assembled on an *ad hoc* basis from preformed materials already present in the cell because their development is not affected by cyclohexamide. At a more physiological level, the uterus at term changes from being a multiunit muscle to a single unit; however, one difficulty in assigning cell–cell transmission to increased numbers of gap junctions is that electrical changes precede the structural.

With respect to human asthma, it has been suggested that the increased excitability of the airways, typical of that condition, stems from the smooth muscle changing its properties from multiunit to single unit. Akasaka et al. (1975) have demonstrated the presence of strong action potential activity in the intact airways of human asthmatics. They employed an extracellular electrode system. Their observation is important and needs to be confirmed. Akasaka's records also demonstrate action potentials in controls, although much less in number than in the asthmatic. Thus, it seems that it is not so much a conversion of ASM from multiunit to single unit in these patients as from single unit with weak activity to single unit with a stronger activity.

Peg-and-Socket Junctions

Such junctions have been described by Burnstock (1979) in intestinal smooth muscle. They are formed by a peglike extension of one cell into another. They do not appear to possess nexus or gap junction properties. Their precise function is not known, but they could serve to couple cells mechanically.

Mitochondria, Golgi Bodies, Lysosomes, and Nuclei

Mitochondria. We (Stephens and Wrogemann, 1970) have reported that mitochondria in ASM resemble those seen in skeletal muscle. Mitochondria have been classically described as situated at the nuclear poles in smooth muscle. This, however, is not always the case, and they may be found almost anywhere in the cytoplasm, from the sarcolemma to the nuclear membrane. Aggregations of glycogen granules can often be seen in their vicinity, presumably acting as an energy substrate. Fat globules are occasionally found in the same location. The two questions most often raised about mitochondrial function are, What is their quantitative role in energy production and what part do they play in excitation-contraction coupling? With respect to energy production, we showed that smooth muscle mitochondria function just like those of striated muscle. Their phosphorylation rates and ADP:0 ratios are quantitatively in the lower normal range of those of striated muscle. They employ all the substrates that skeletal muscle uses. A major difference is that the amount of mitochondrial protein present in a smooth muscle cell is only one tenth of that in skeletal. Hence, the phosphorylation capacity, which is defined as the amount of ATP synthesized oxidatively per

unit weight of muscle, is only one tenth of that in skeletal muscle, and even less in cardiac. Thus, oxidative phosphorylation supplies less energy to the smooth muscle than it does to striated muscle. The former also relies to a greater extent on anaerobic glycolysis. One interesting feature to emerge is that the energy supply may be compartmentalized. It has been reported (Paul et al., 1976) that even though oxidative phosphorylation supplies energy predominantly for the needs of the membrane, glycolysis powers the contractile machinery.

We have also reported (Stephens and Vogel, 1972) that with tissue hypoxia ASM mitochondria develop irreversible defects in their phosphorylation capacities. Hence, even though the muscle may recover mechanical function on reoxygenation, it does so with an obligatorily heavier reliance on glycolysis, and in all likelihood operates with reduced reserve.

The notion that mitochondria are importantly involved in excitation–contraction coupling was considered some years ago. It was thought they could act as a source for calcium, however, this was based on *in vitro* data. It is now known that at physiological levels of calcium the mitochondria could not act as sources of activator calcium. When calcium levels are pathologically increased they may well act as calcium sinks.

Golgi Bodies

These are generally found at the nuclear poles; however, no functional studies of the airway smooth muscle Golgi apparatus have yet been carried out.

Lysosomes

These are rarely seen, but may be encountered in increased numbers in chronically hypoxic tissues.

The Nucleus

This is typically cigar-shaped, single, and centrally located. It possesses well-defined chromatin and a nucleolus. A nuclear membrane with pores surrounds the nucleus. During isotonic shortening the nucleus shows marked twisting, and this feature is used to identify shortened cells in tissue.

Innervation of Airway Smooth Muscle

It has already been pointed out that the nerve terminals run in the connective tissue lying between the smooth muscle cell bundles and that they do not penetrate into the depths of the bundle. Their types and characteristics have been described by Kirkpatrick (1975), Suzuki (1976), Richardson (1979), Irwin (1980), Daniel (1986) and others (Dahlstrom et al., 1966; El-Bermani et al., 1970; O'Donnell and Sarr 1973).

The nerves are all nonmyelinated and exist as bundles of axons and axonal varicosities with synaptic vesicles. Axons occur with a frequency of 3–10 per muscle cell bundle, and are partially or completely surrounded by Schwann cell sheaths. Our own studies, however, show that there is approximately one axon for every 10 muscle cells; we have no explanation for the discrepancy.

The autonomic nerves that control ASM generally show a pattern that consists of sensory afferent nerves originating in the epithelium of the airways, the lung parenchyma, and the muscle. Efferent fibers may be myelinated or nonmyelinated and end in the vagal nuclei. Afferent fibers run to the muscle cells and glands and originate in ganglia. The latter are controlled preganglionically from the vagal nuclei and are part of the parasympathetic nervous system. Ganglia are situated close to the effector organ, lying external to the smooth muscle and the cartilage. The preganglionic fibers of the sympathetic nervous system leave the spinal cord and synapse with prevertebral ganglia. Postganglionic fibers emerge from the ganglia and are said to innervate the airway smooth muscle glands and pulmonary blood vessels.

Some controversy exists as to the control exerted by the adrenergic nervous system. Although the parasympathetic nerves are the major motor control system for ASM, there is no certainty as to whether the sympathetics are responsible for relaxation. There is no doubt that β-adrenoceptors are present in the airways and that β-adrenoceptor agonists are powerful bronchodilators. The extent receptor function is controlled by adrenergic nerves is not clear. Richardson (1975) reports there is no neural control and that the major relaxing system is that of the so-called nonadrenergic noncholinergic inhibitory system. Sympathetic nerves are said to be mainly destined for vascular smooth muscle when found traversing the airway.

There is considerable species variation with respect to the adrenegic nerve (Coburn and Tomita, 1973; Richardson and Bouchard, 1975; Irvin et al., 1980). In the cat there is a rich adrenergic supply of nerves to the smooth muscle of the airways. In the guinea pig (Coburn and Tomita, 1973), however, the adrenergic innervation is mainly to the proximal trachea. It used to be claimed that less variation existed in cholinergic innervation to the airways than in the adrenergic; however, this has had to be modified in view of the recognition of a nonadrenergic noncholinergic excitatory system in some species. This acts either directly or by an axon reflex. The putative transmitter is substance P and the system is capsaicin-sensitive. Furthermore, it appears that although the proximal airways are under strong cholinergic control, the small peripheral airways are controlled via leukotrienes, prostaglandins, histamine, or serotonin.

Daniel et al. (1986) have identified two types of axonal varicosities in the dog trachealis.

Nerves that contain small agranular vesicles (SAV) are by far the most numerous and are cholinergic. They account for about 50% of the total axonal pool. Figure 5 shows an axon lying just below and to the left of a smooth muscle cell. The SAV have been labeled ACh (acetylcholine-containing) in this picture. These vesicles are about 50–70 nm wide. Nerves containing adrenergic vesicles (small granular vesicles or SGV) are very few. SGV are about the same size as the

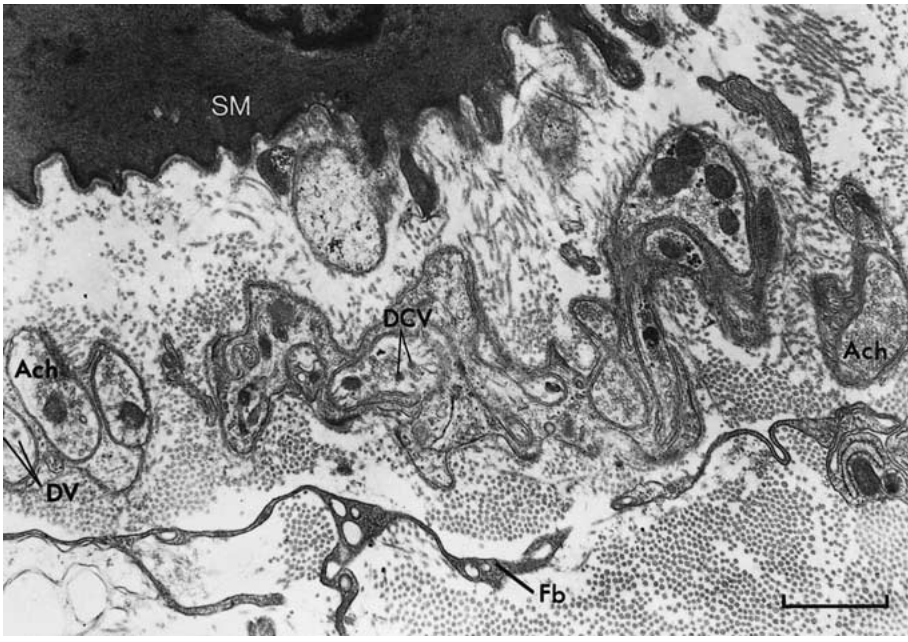

Fig. 5. Longitudinal section of canine tracheal smooth muscle showing an axon with small granular vesicles containing acetylcholine (ACh). Dense cored vesicles (adrenergic) are also seen. SM = smooth muscle cell (mag × 26,000).

cholinergic vesicles. Large granular vesicles (LGV) are occasionally seen with dense cores. The diameter of these vesicles is about 100 nm. Large clear vesicles (LCV) are also seen. All these vesicles can exist in various combinations.

Coburn and Tomita (1973) first reported the existence of a nonadrenergic inhibitory noncholinergic (NANCI) nervous system in the airways of the guinea pig. It was regarded as purinergic. Similar nerves exist in the gastrointestinal system, where their effect is also inhibitory. They are also present in the urinary bladder, but their role is excitatory. The NANCI system appears to develop in conjunction with the cholinergic excitatory system and precedes that of the adrenergic system. The chemical mediator was initially felt to be ATP or ADP, so the system was termed purinergic; however, at least for the airways, this notion has been abandoned and the currently favored neurotransmitter is vasoactive intestinal polypeptide (VIP). The axon profiles of this system are distinct from those of the other nerves in that they contain large (180–220 nm wide) opaque vesicles that are neither destroyed by 6-hydroxydopamine nor depleted by reserpine. As pointed out before, in postmortem human material, Richardson and Beland (1976) have found no evidence for the existence of adrenergic inhibitory nerve fibers, but have demonstrated pharmacologicaly the presence of nonadrenergic inhibitory nerves in the smooth muscle of the human trachea and bronchi. We have detected large dense cored vesicles in about 2% of the axons we counted in multiple sections of canine airway smooth muscle; however, we have not been able

to pharmacologically detect the presence of the nonadrenergic noncholinergic inhibitory system in the dog's trachealis. The key questions are whether the system is active *in vivo* and whether there is direct evidence for its existence. At least in the cat, Irvin et al. (1980) have provided good pharmacological evidence that such a system is operative in the living animal. There is evidence that the system also exists in humans but is weakly operative. The pharmacological evidence is indirect and inconclusive. A specific antagonist is needed.

Do Sarcomeres Exist in Smooth Muscle?

Ever since it was known that myosin is contained in smooth muscle cells, the idea has devloped that myosin filaments resembling those of striated muscle also existed in the smooth muscle; however, these were destroyed in preparing the section for microscopy. If this could be avoided, then perhaps a sarcomeric pattern would also be detected in the smooth muscle.

Several years were to elapse before appropriate techniques were developed to demonstrate organized thick myosin filaments. Figure 2 (canine trachealis section) shows thick filaments in the second cell from the top. One is seen in its entirety and is about 2 μm long. Gabella (1976) and Somlyo (1980) have made careful studies of these filaments in taenia coli and vascular smooth muscle cells, respectively. Their measurements indicate that the average length of the filament is 2 μm, longer than that of striated muscle (1.65 μm). Another difference is that smooth muscle filaments lack the central bare area that is typical of striated muscle myosin filaments. Myosin filaments have been synthesized *in vitro* from smooth muscle myosin. The structure of the smooth muscle myosin molecule has also been studied with the electron microscope and confirmed that it is double-headed and possesses a long rodlike tail.

The structure of the smooth muscle actin molecule and of the thin filament has been more highly conserved and resembles that of striated muscle; the same holds for its biochemical properties. The ratio of actin to myosin filaments is about 13–15:1, which greatly exceeds the 6:1 ratio of striated muscle. The orientation of cross-bridges is said to be side-polar and not bipolar, as in striated muscles. This orientation of bridges would enable the greater shortening of smooth muscle, vis-à-vis that of striated.

The idea that sarcomeres may exist in smooth muscle arose from studies of dense bodies by Fay et al. (1984), who employed immunohistochemical techniques. Although dense bodies and dense bands have been recognized for many years, they were thought to be randomly distributed throughout the cytoplasm; however, delineation of the dense bodies was considerably improved by using α-actinin (a major component of dense bodies) antibodies. Computer imaging and analysis showed that these bodies existed in orderly arrays that demarcated sarcomerelike units. They were analogous to Z discs but were not complete structures. A series of dense bands is seen in Figure 6. Stability for the putative Z discs is provided by long arcuate cytoskeletal desmin fibers that extend from one dense body to the next, as indicated by the arrowheads.

Fig. 6. Longitudinal section of portal vein smooth muscle briefly sinned with saponin and fixed in the presence of tannic acid. Actin filaments (small arrows) insert on both sides of the dense bodies (db) and run to the myosin filaments. The 10 nm filaments (arrowheads) are closely associated and surround the dense bodies (see db on the right). The 10 nm filaments connect the dense bodies rather than running parallel to the sarcomere unit. (Source: From Somlyo et al. (Stephens NL, ed) Smooth Muscle Contraction, Marcel Dekker, New York 1984, with permission.)

Thin filaments (shown by arrows) enter the dense bodies from one side and emerge from the other exactly as they do in Z discs of striated muscle. The actins show polar reversal on traversing the dense body. In between the actin filaments Figure 6 shows well-defined thick filaments. Even though there is a long way to go from these ill-defined minisarcomeres to the beautiful, orderly arrays of striated muscle, all sarcomeric ingredients nevertheless appear to be present in smooth muscle. It is on these, admittedly tenuous, grounds that we feel the sarcomeric sliding filament cross-bridge theory of contraction can be applied to the smooth muscle. Hellstrand and Johansson's (1979) mechanical data suggest that rotation of the head may also be incorporated into the theory.

Using actin and myosin antibodies, Groschel-Stewart et al. (1975) have demonstrated remarkably clearcut striations in smooth muscle cells. Because Gabella (1976) considers these to be surface striations, more work is needed to decide the issue.

Electrophysiology of Airway Smooth Muscle

This has been reviewed before by us for canine tracheal smooth muscle. Suzuki et al. (1976) have also delineated the electrical properties of the same tissue in detail. Kirkpatrick (1975) has described the electrophysiology of bovine tracheal smooth muscle. We will summarize by saying that in keeping with its intermediate unit–type of muscle properties, canine tracheal smooth muscle possesses a steady membrane potential of about −47 mV ± 2.4 (SE). As stated before, spontaneous action potentials are seen only under abnormal conditions. Agonists produce graded depolarization and the mechanical threshold differs from the equilibrium membrane potential by only 3–4 mV [22]. Current-voltage plots reveal considerable rectification due to increased potassium conductance. This accounts for absence of action potentials. Current injection experiments using an Abe and Tomita–type bath system (1968) show that the space constant is about 1.6 mm.

K^+ Channels

Airway smooth muscle shows a graded depolarization to the application of KCl; no action potentials are seen due to rectifying K^+ channels outwardly. Membrane potassium conductance accounts for this electrical stability.

Whole-cell patch clamp techniques indicate that several voltage-sensitive K^+ channels are present in the ASM cell. The lack of an effect on the K^+ current by Ca^{2+} channel block (with charybdotoxin) indicates the current is carried by non-$K^+(Ca^{2+})$ channels. In fact, these are the so-called delayed rectifier channels. With respect to anomalous rectification in AMS, it is likely that the delayed rectifier currents are more important.

To complete the tally, mention must be made of K^{ATP} channels. These are present in VSM and ASM. They are thought to be the site of action of cromakalim and pinacidil, which are reported to relax blood vessels. Glibenclamide, a sulfuryl urea drug, is said to block these K^+ channels. In human subjects,

cromakalim inhibits histamine-induced bronchoconstriction and can protect again nocturnal asthma. The action of cromakalim is to open K^+ channels that are normally kept closed by ATP.

Ca^{2+} Channels

So-called transient (T) and long-lasting (L) Ca channels have been reported in VSM membranes (Bean et al., 1986). In ASM, the main channels are T-type (Mitra and Morad, 1985: Klockner and Isenborg, 1985; Kotlikoff, 1988) as suggested by the rapid inactivation of the Ca^{2+} current. The picture is not yet clear, however because some similarities to L channels also exist.

Kotlikoff (1989) has reported that Ca^{2+} currents are smaller in amplitude than K^+ currents.

That smooth muscle membrane Ca^{2+} channels show some differences in behavior when compared with cardiac or nerve cells is not surprising because Schmid et al. (1986) showed that smooth muscle Ca^{2+}-channel proteins react differently to antibodies against the other two.

Excitation–Contraction Coupling

Coupling in smooth muscle is of two types, electromechanical and pharmacomechanical (Somlyo and Somlyo, 1968), the latter developing when stimulation is effected by pharmacologic agents and is associated with either minimal or no membrane depolarization. Coburn (1977) has shown that in such coupling (induced by acetylcholine, for example) injection of repolarizing current does not reverse the contraction. Another characteristic is that pharmacomechanical coupling can be seen even when extracellular Ca^{2+} concentration is zero and must therefore depend upon intracellular stores. Finally, Ca^{2+} antagonists that block voltage-dependent Ca^{2+} channels do not reverse acetylcholine-induced contractions.

Electromechanical coupling is mediated by voltage-operated channels (VOC). The parameters regulating the quantity of Ca^{2+} influx are frequency and duration of channel open times. As mentioned earlier, there are two types of Ca^{2+} channels: so-called T-type channels, which are inactivated quickly, and L-type, which are inactivated very slowly or not at all (Ohya et al., 1988). These show the same properties as those in striated muscle cells. The L-type channels are activated at voltages ranging from -20 to $+40$ mV, and they are blocked by dihydropyridine-sensitive Ca^{2+} channel blockers. The T-type channels are activated at more negative voltages and do not respond well to dihydropyridine antagonists.

In canine ASM specifically, Kotlikoff (1988) has shown that T channels display their usual properties but are difficult to characterize, perhaps due to the limitations of the patchclamp technique.

The phenomenon of anomalous rectification of the ASM membrane has been already mentioned. It is dependent on conductance of $K^+(Ca^{2+})$ channels.

Kotlikoff has suggested that a K^+-independent Ca^{2+} conductance is also involved. It is this rectification that is responsible for the graded mechanical responses of ASM.

A second messenger is involved with respect to pharmacomechanical coupling. This is IP_3 liberated by ligand activated phospholipase C, as reported by Baron and Coburn (1987) and Baba et al., (1988). The subject of inositol phospholipid metabolism in smooth muscle (including ASM) and of the role of IP_3 in releasing Ca^{2+} from intracellular stores has been well reviewed by Baron (1989).

In the course of inositol phospholipid metabolism, diacylglycerol is also produced and may contribute to the coupling process by activating protein kinase C (PKC) which phosphorylates cytoskeletal and other unidentified polypeptides resulting in contraction. It is interesting that PKC does not activate the myosin light chain phosphorylation pathway; if anything, it is inhibitory.

Mechanical Properties of Airway Smooth Muscle

Length–Tension Relationships

Isometric studies of tension and length provide information about the ability of the muscle to stiffen and support loads, as well as about muscle elasticity. Length–tension curves obtained by supramaximal electrical stimulation of isolated isometric canine tracheal smooth muscle strips are shown in Figure 7. The resting tension curve shows the shape expected of complex biologic tissues; it results from the presence of collagen and elastin (Roach and Burton, 1957). Because smooth muscles generally possess variable degrees of resting tone, passive length-tension curves are obtained after treatment with appropriate pharmacologic relaxants or metabolic inhibitors of energy production. Canine TSM demonstrates stress-relaxation. Its magnitude is a direct function of length change and the period of time the muscle is held isometric at high tensions. Length change in excess of 25% of the initial length results in stress-relaxation. Because of stress–relaxation, length–tension curves show hysteresis; repeated cycling of tissue length narrows the loop.

Figure 7 also shows total and active tension curves. Active tension is the important one to consider because it provides insight into the working of the contractile element of the muscle. The curve shows a maximum at a unique length that is defined as optimal length (l_o). In skeletal muscle l_o has the additional quality of representing the muscle's *in vivo* length. It has recently been determined that this is so for the TSM (Moreno et al.). The maximum active tension (P_o) elicited is 1.10 kg/cm^2 (1.10×10^5 N/M^2) + 0.059 (S.E.). This value of P_o is obtained when the bathing medium is at 37°C and has a 2 mM calcium concentration; when the latter is raised to 4.75 mM, P_o increases to 1.980 kg/cm^2 + 0.123 (S.E.), which represents an 80% increment (Stephens et al., 1983). When the concentration is raised to beyond 4.75 mM, P decreases presumably because of the stabilization of the muscle cell membrane. Both smooth (Stephens, 1975) and

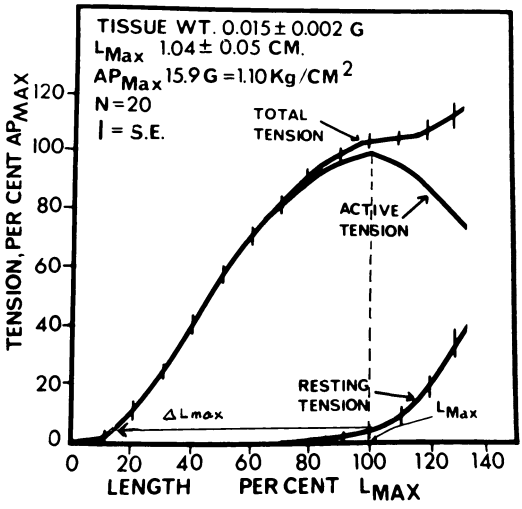

Fig. 7. Mean LT curves (± SE) for canine trachealis. Note: Full curve not shown.

heart (Jewell, 1974) muscle differ from skeletal muscle in which there is no increase of P_o (at l_o) with Ca^{2+} — concentration greater than 2 mM. The TSM data confirm the observation by Aksoy et al. (1982) that smooth muscle cross-bridges develop the same force as those of skeletal. Because the former muscle possesses only one-fifth the myosin of the latter, this performance is remarkable.

Another noteworthy feature is the ability of the TSM to "supercontract" i.e., to shorten much more than skeletal muscle, which can only shorten to 65% of l_o; the TSM shortens to 10% of l_o. The mechanism enabling this is unknown, nor is it easy to see what is its *in vivo* significance. Macklem (personal communication) has speculated that the capacity for supercontraction raises the question as to why severe asthmalike bronchoconstriction does not occur normally. He suggests that shortening is abbreviated by the activation of a nonadrenergic, noncholinergic inhibitory nervous system. We believe that it is the phenomenon of reduced activation of the muscle at short lengths ($l < l_o$), discussed later that is responsible. Another concept put forward by Macklem (personal communication, 1991) is that alteration in the elastic recoil forces that the lung parenchyma exerts on the airways regulates bronchoconstriction.

In length–tension curves, the maximum isometric tetanic tension developed at any length is influenced by the history of the contraction. We have reported (Stephens and Van Niekerk, 1977) that isometric active tension curves differ from those derived from freeloaded or afterloaded contractions. At any given length, the tension developed by muscles that contracted is always less than that of muscles in which no shortening occurred.

Reduced Activation at Short Lengths. Rudel and Taylor (1971) observed that at $l < l_o$, there is reduced mechanical activation in single skeletal muscle fibers. Jewell (1974) has reported that the same phenomenon exists in cat heart whole papillary muscle. Siegman (personal communication, 1986) has obtained similar findings for smooth muscle. Figure 8 shows two active tension (P) versus length (l)

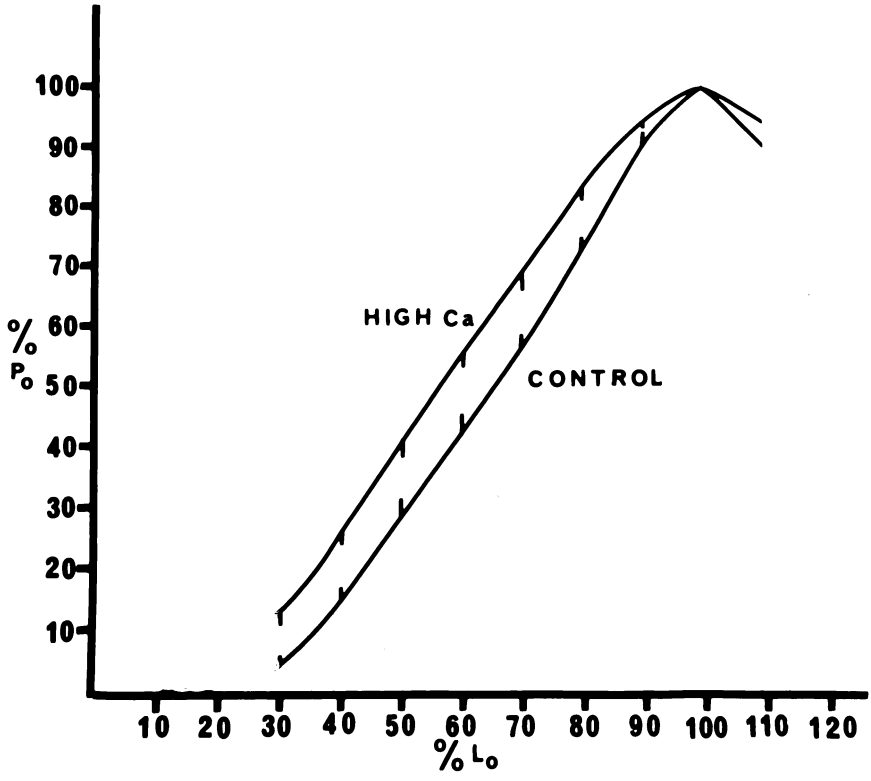

Fig. 8. Active length-tension curves shown in percentized units. For the control curve 2.0 mm Ca^{2+} was used, whereas a 4.75 mM concentrations was used for the "high Ca" curve.

curves. Length and tension are expressed as of l_o and P_o respectively. The curve to the right was obtained from muscles incubating in a bathing medium containing 2 mM Ca^{++} at 37°C. The curve to the left was elicited from a muscle incubating in medium containing 4.75 mM Ca^{2+}. The shift to the left indicates that at lengths between 40% l_o and 85% l_o the muscle was not maximally activated. The mechanism underlying this phenomenon in smooth muscle is not known, but it suggests that the muscle could be mechanically unstable at these lengths. Another speculation is that as the smooth muscle shortens (e.g., during expiration) the airway undergoes critical closure. The associated reduction in activation would minimize this.

Force–Velocity Relationships

Length–tension curves are of limited value because they only deal with static conditions. They do not enable one to assess the power production of the muscle. For this, force–velocity curves are needed. A mean force–velocity curve, derived

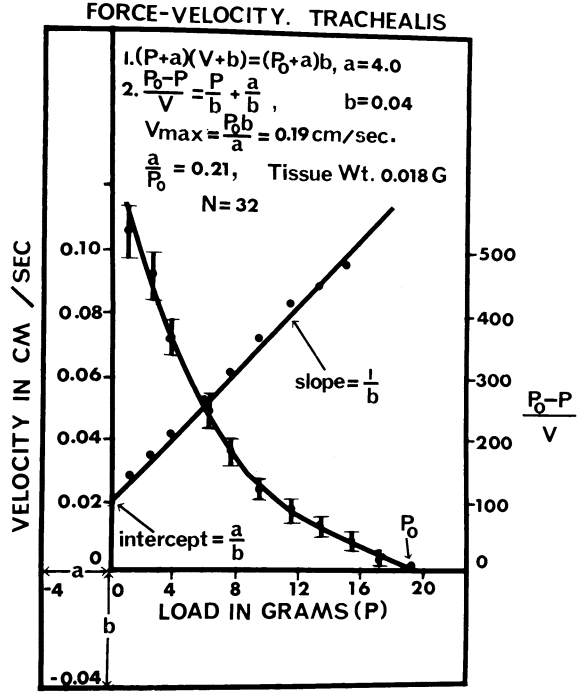

Fig. 9. Force-velocity curves for canine trachealis, measured by after-loaded isotonic methods. Means and SEs are shown. Plotting $(P_o-P)/V$-shown in right-hand ordinate—against load (P) linearized the rectangular hyperbola. From the slope and intercept constants for the F–V curve was obtained $(P+a)(V+b) = (P_o+a)b$ is the classical Hull equation. P = load (equal to force); P_o = maximum isometric force: a and b are asymptote values; a has units of force and b has units of velocity.

from records of isotonic afterloaded shortening in TSM, is shown in Fig. 9. It is fitted by Hill's equation (Hill, 1939):

$$(P + a)(v + b) = (P_O + a)b$$

where v is the maximum velocity for a given load

a = a constant with units of force and an index of numbers of force-generating sites in the muscle's cross-section

b = units of velocity and is an index of the rate of energy liberation or of actomyosin ATPase activity.

These constants can be calculated from the slope $(1/b)$ and intercept (a/b) of a plot of $(P_o - P)/v$ versus P (solid line in Fig. 9), which is a linearizing transform of Hill's equation. There is doubt as to the usefulness of this equation because the a constant appears to be load dependent; however, Woledge (1985) has shown that a is a true constant for smooth muscle. The final constant

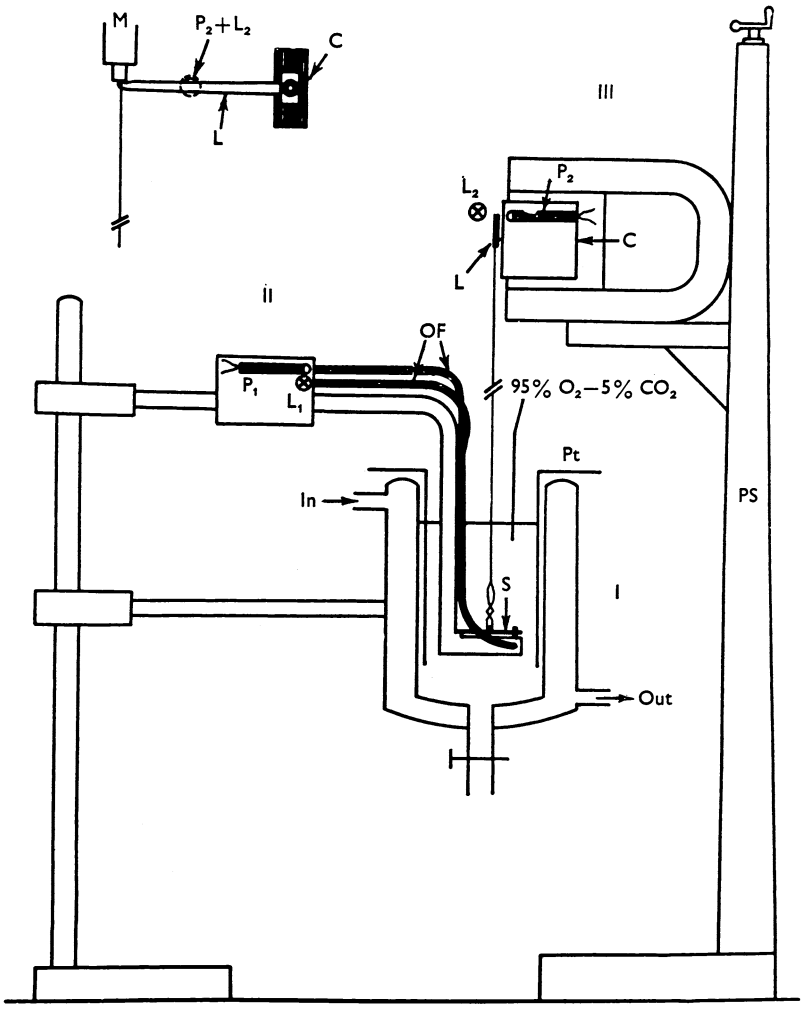

Fig. 10. Vertical section of the apparatus. Panel I: cylindrical glass muscle bath with double wall; In = inlet; out = outlet; for temperature control; Pt = platinum electrodes. Panel II: force transducer; P_1 = silicon photodiode; L_1 = miniature lamp; OF = optical fibres; S = spring with a shutter and muscle clip. Panel III: Electromagnetic lever system; P_2 = silicon photodiode; L_2 = miniature lamp; L = lever; C = coil. Insert (upper left), front view of electromagnetic lever system: M = micrometer stop; PS = Palmer stand.

obtained from the data is V_o, which is the velocity of shortening at a hypothetical zero load. V_o is obtained from the equation $V_o = P_o b/a$. The curve shows that P_o is not too dissimilar from that of skeletal muscle; however, V_o is almost fifty times slower.

Changes in V_o in a given muscle suggest changes in actomyosin ATPase activity. Antonissen et al. (1971) have shown that V_o is increased in TSM from a canine

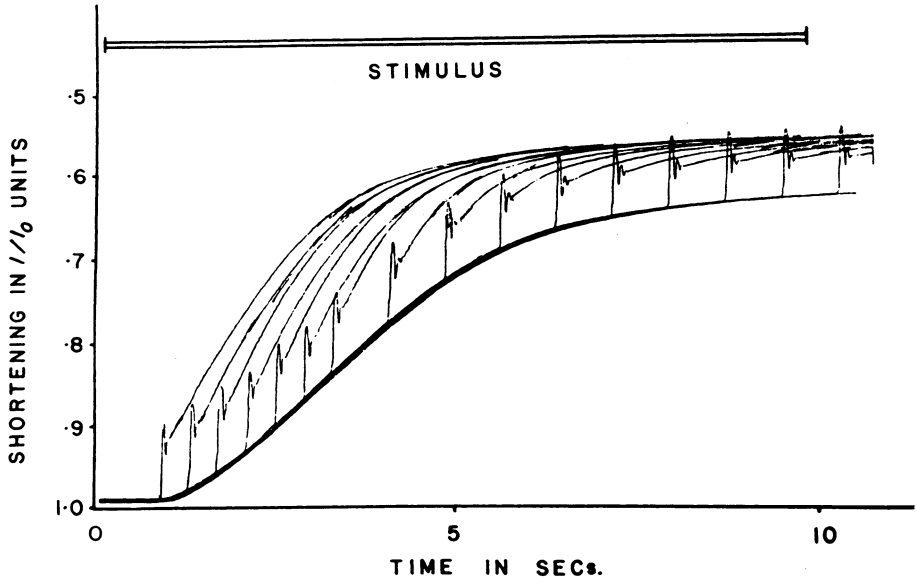

Fig. 11. Oscilloscope records obtained from a single typical experiment out of a sample of 20. Shortening in normalized units is plotted against time in seconds. The lowest curve, which is sigmoidal, represents preloaded isotonic shortening. The quick-releases made were always to zero load. At different times during shortening the preload was reduced to zero within 3 msec. Optimal clamping was determined for each experiment. Each zero load clamp shows two phases: an initial rapid transient stemming from recoil of the muscle's series elastic component, followed by a few artefactual oscillations and then a slow transient. The maximum slope of this latter phase provided the maximum velocity of shortening (V_o) for the particular instant in time. Progressive diminution of this velocity with time is evident.

model of allergic bronchospasm. This is important because it suggests that the underlying alteration is in the ATPase and points the way to biochemical research.

It must be pointed out that estimation of V_o involves mathematic or graphic extrapolation. Brutsaert et al. (1971) have suggested such extrapolations could be inaccurate and have devised a method for directly measuring velocity at zero load by applying an abrupt zero load clamp. In this way, velocity points have been obtained between zero load and the preload that was needed to set the muscle at its l_o. Using a muscle lever built by Brutsaert for us, we have obtained velocity data points for this range of loads as shown in Figure 10. Analysis of the data obtained demonstrates the V_o measured by analysis of the conventional afterloaded data or of the entire set of afterloaded and load-clamped data, or by direct measurement (zero load), is the same. From these results, two useful conclusions follow: the conventional analysis of afterloaded isotonic shortening curves is valid for TSM, and V_o can be accurately obtained by a single (zero load clamp) measurement.

The conventional analysis of force–velocity curves yields erroneous results for high load values because the bridges responsible for force development seem different from those responsible for the velocity of shortening. Even though the

values of velocity at low loads are accurate, those at high loads are not. This problem is resolved by measuring force–velocity curves for the two types of bridges separately. This is facilitated by using so-called abrupt load-clamping techniques.

Normally Cycling and Latch (or Slowly Cycling) Bridges

Discoveries by Dillon et al. (1981) have shown that the skeletal muscle approach cannot be applied when analyzing the mechanical properties of smooth muscle because of the differences in cross-bridges for the two types of muscles. Two types of bridges are activated sequentially in smooth muscle. Those activated first manifest maximum cycling activity and are called *normally cycling* cross-bridges. They are activated by phosphorylation of the 20,000-dalton myosin light chain, which enables actin activation of myosin ATPase activity. Calcium-calmodulin activation of myosin-light-chain kinase is responsible for the phosphorylation. The normally cycling cross-bridges are soon replaced by very slowly cycling bridges that consume about one quarter the energy of the former. They have been termed *latch* bridges and reduce the muscle's velocity by retarding the normally cycling cross-bridges; however, this notion is disputed and some believe what is really happening is that the normally cycling cross-bridges slow progressively with time and latch bridges do not develop. According to this view, these bridges should be termed *slowly cycling* cross-bridges (Butler et al. 1983). Results of studies of the energetics of smooth muscle contraction by our group support the notion.

We have shown that normally cycling cross-bridges and latch bridges also exist in canine (Stephens et al. 1980) and murine (Xu et al. 1980) TSM and in the canine coronary artery (Wang et al. 1988) and saphenous vein (Wang and Stephens, 1989).

These cross-bridges are recognized by their unloaded shortening velocities. Figure 11 shows the results from the application of so-called zero-load clamps to a tracheal muscle shortening isotonically under a load just sufficient to stretch it to its l_o. The loads were applied at 0.5-second intervals using a special electronic muscle lever system devised by Brutsaert and colleagues (1971). The response shown in the figure consists of a rapid transient resulting from elastic recoil of the series elastic component followed by a slow transient due to shortening of the contractile element. The maximum slope of this component is represented by V_o. Scrutiny of the slow transients demonstrates a progressive decline in V_o. The low V_o is due to latch-bridge activity.

These data confirm that normally cycling and latch bridges are also present in ASM. Analysis has also shown that, in the normally preloaded muscle, 75% of the isotonic shortening is due to normally cycling cross-bridge activity and that most of the maximum isometric force developed is due to latch-bridge activity. It almost appears that smooth muscle has developed discrete, dedicated cross-bridges—at least in a functional sense—to its two major activities of shortening and stiffening. The implications are fairly important because they indicate (e.g., in asthma) that in order to elucidate the mechanism of bronchoconstriction it is the

normally cycling cross-bridges that must be studied (i.e., studies must be conducted within the first 2–3 seconds of isotonic contraction).

The Series Elastic Component

Mechanical records of smooth muscle contraction indicate that its series elastic component (SEC) is longer (or more compliant) than that of striated muscle. We have published the properties of the SEC of TSM (Stephens and Kromer, 1971). The studies showed that when the isometric muscle developed a force equal to P_o the internal elongation of the SEC was 7.5% l_o. Similar values have been reported for VSM (Johansson, 1978), but on the whole, larger values are seen in the majority of smooth muscles. Alterations in these properties in hypoxia (Kroeger and Stephens, 1971; Stephens, 1972) were correlated with changes in P_o, suggesting that the SEC resides in active components, most likely the cross-bridges.

Seow and Stephens (1987) have studied the time dependence of series elasticity in canine tracheal smooth muscle and reported that the stress–strain curve for the SEC of tracheal smooth muscle was obtained by quick releasing the muscle from isometric tension to various afterloads and measuring the elastic recoils (SEC lengths) at a specific time after stimulation. A family of such curves was obtained by releasing the muscle at different points in time during contraction. Stiffnesses of the SEC (slopes of the stress–strain curves) at a specific stress level calculated from these curves (constant-stress stiffness) showed a significant difference from one another. The same difference can also be characterized by the slope of the linear stiffness–stress curve, the constant A. The constant A during a 10-seconds isometric contraction was maximal at 2 seconds; it then decreased with time. This stiffness behavior is only seen when the effect of stress is held constant or eliminated. If stress is allowed to increase with time as it does during a tetanus, then stiffness appears to increase monotonically. The SEC stiffness during active contraction was found to vary within the boundaries of the stiffness of muscle in rigor (upper limit) and that at resting state (lower limit).

They also studied changes of tracheal smooth muscle stiffness during an isotonic contraction and relaxation (Seow and Stephens, 1989). This was measured by applying small force perturbations to the muscle and measuring the resulting length perturbations. The quick, elastic length transient was taken as the change in length of the SEC (ΔL). The force perturbation was a train of 10-Hz rectangular force waves varying from 0 to 10% maximum isometric tension (P_o) in magnitude ($\Delta P = 10\%\ P_o$). Stiffness of the SEC was estimated by the ratio $\Delta P/\Delta L$. The change in SEC stiffness with respect to the change in muscle length was further studied by obtaining the stress–strain curves of the SEC at different muscle lengths using the load-clamping method. The clamps were applied at a fixed time (10 seconds after stimulation). Length of the muscle 10 seconds after contraction was controlled by the magnitude of the isotonic afterload. It was found that the apparent SEC stiffness increased as muscle length decreased. This stiffness in-

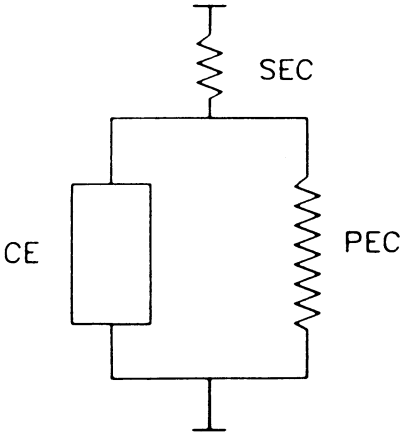

Fig. 12. Schematic representation of Voigt's model. SEC = series elastic component; PEC = parallel elastic component; CE = contractile element.

crease is not likely due to an increase in the number of attached cross-bridges, but probably to the gradual diminution of the SEC length itself during muscle shortening.

The Parallel Elastic Component/Internal Resistance to Shortening

This is an area of ASM research, and of smooth muscle in general, that has been totally unexploited. The few studies of smooth muscle shortening that have been undertaken have been conducted during the course of studies of velocity with the tacit assumption that a muscle shortening at greater velocity will shorten to a greater extent. This would be true if shortening was unimpeded in its entirety; unfortunately, this is not so. For example, if a muscle strip is stimulated, and, at maximum shortening, the stimulus is removed, the muscle relaxes precisely to its original length. It is as if there was an inert internal resistor (IR) that became compressed during shortening and recoiled passively during relaxation. In a sense the IR is a component of the parallel elastic component (PEC). Examination of the resting tension curve in Figure 7 shows that resting tension is zero at 0.80 L_{max} (or 0.81 L_o). At lengths greater than this the resting tension increases to support the weight of the passive muscle. This part of the curve (i.e., from 0.8 L_o upwards) represents the tension-extension property of the PEC. Voigt's model (Fung, 981) of the muscle incorporating PEC, SEC, and CE is shown in Figure 12. In ASM, it is clear that because resting tension at L_o is low, very little shortening reduces it to zero, which represents the neutral point of the spring representing the PEC. Any shortening beyond this produces compression; the extent of compression is a function of the elasticity of the spring. It is this elasticity that will limit muscle shortening, no matter what the velocity of shortening. Study of the IR is just as important (if not more) as that of the CE (velocity of shortening) in elucidating regulation of airway caliber and the pathogenesis of asthma. It is easy to see that increased complicance of the IR would result in increased shortening ability of the ASM

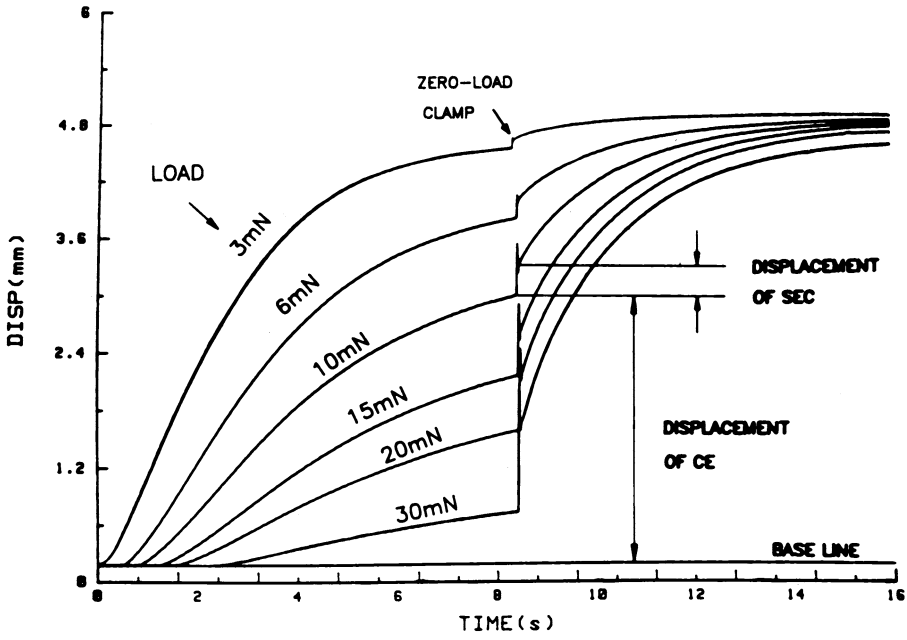

Fig. 13. Experimental records of shortening versus time from a strip of canine trachealis. A range of load clamps (3–30 mN) was applied at 8 seconds.

and thus account for allergic bronchoconstriction. The point is crucially important as the biochemistry of the altered resistance to shortening is quite different from that of the velocity of the CE.

Stephens (1988) developed a method for delineating the tension–compression curve of the IR. He reasoned (Fig. 12) that if the SEC load is suddenly reduced to zero, the load on the CE would also be zero which would then shorten at V_o. With further shortening PEC compression would internally load the CE whose velocity would drop accordingly. This drop in velocity would be an indirect index of the elastic property of the PEC. The method or analysis requires one critical assumption. The FV curve for the CE is the same regardless of whether the loading is internal via the compressed PEC, or external via the SEC.

Maximum V_os at different CE lengths can be measured by abruptly clamping the external load to zero. Figure 13 shows a series of shortening records obtained when the maximally stimulated muscle was permitted to shorten isotonically. At any time, the CE length was a function of load. At the instant shown in the records, zero load clamps were applied. A rapid transient (SEC), followed by a slower CE transient is seen in each record. The maximum velocity developed during the latter phase was then plotted against CE length. Velocity–CE length curves were plotted for a suitable range of CE lengths. In terms of physiologic significance, it is clear that the first 25% of shortening velocity is almost length-independent.

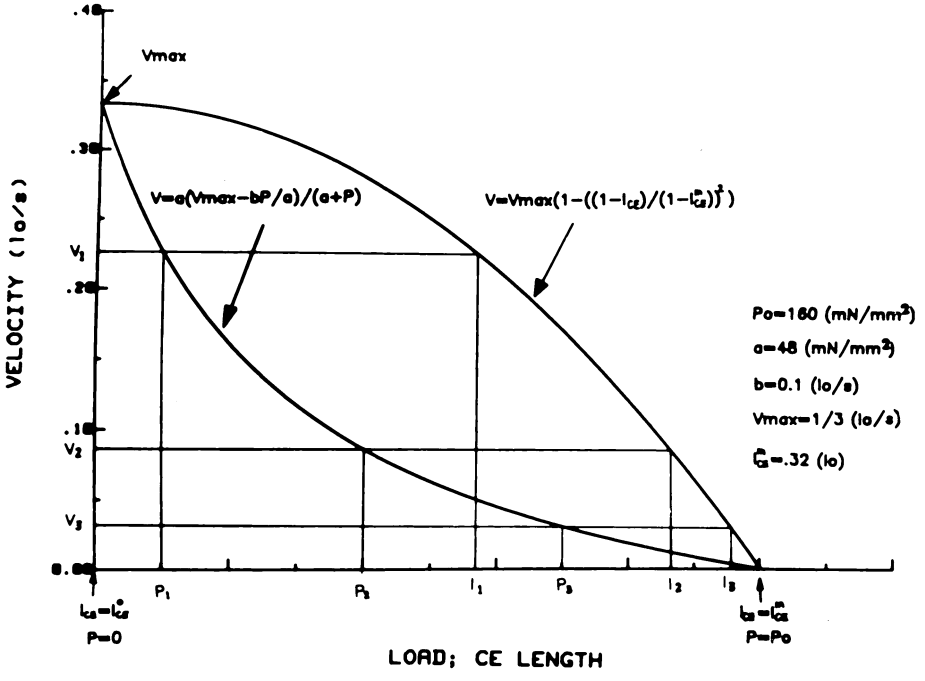

Fig. 14. V_o versus contractile element length curve obtained from data in Fig. 13.

Conventional FV curves were obtained for the same muscle by applying a range of isotonic loads after quick-release at the same moment at which the studies of the internal resistor had been conducted.

Figure 14 shows superimposition of the curve in Figure 14 on the FV curve. From analysis of these curves, tension–compression data for the IR (PEC) were obtained. For example, at a selected velocity, say V_1, the corresponding load, P_1, was read off the FV curve; P_1 represents the load imposed on the Ce by SEC extension by the external load. Reading the velocity–CE length (L) curve (note the abscissa represents both length and load) for the PEC one determines the length at which V_1 develops. The P_1 and L_1 values thus define a point on the tension–compression curve of the IR. Several such points are plotted in Fig. 15 and represent the first report of the tension–compression characteristics of the IR in any muscle. The empirical equation describing the curve is also shown in the figure.

Figure 15 curves for control (CTSM) and sensitized (STSM) canine TSM. The IR of the STSM is clearly more compliant, which could account for the increased bronchoconstriction of asthma. The exact nature of the IR is not known. It could be the intercellular and interfascicular connective tissue or the intracellular cytoskeleton. Only experiments on single cells will decide the issue. Experiments in single cardiac myocytes suggest it is the cytoskeleton (ter Keurs and Iwazume, 1988) to a minor degree and extracellular connective tissue to a major.

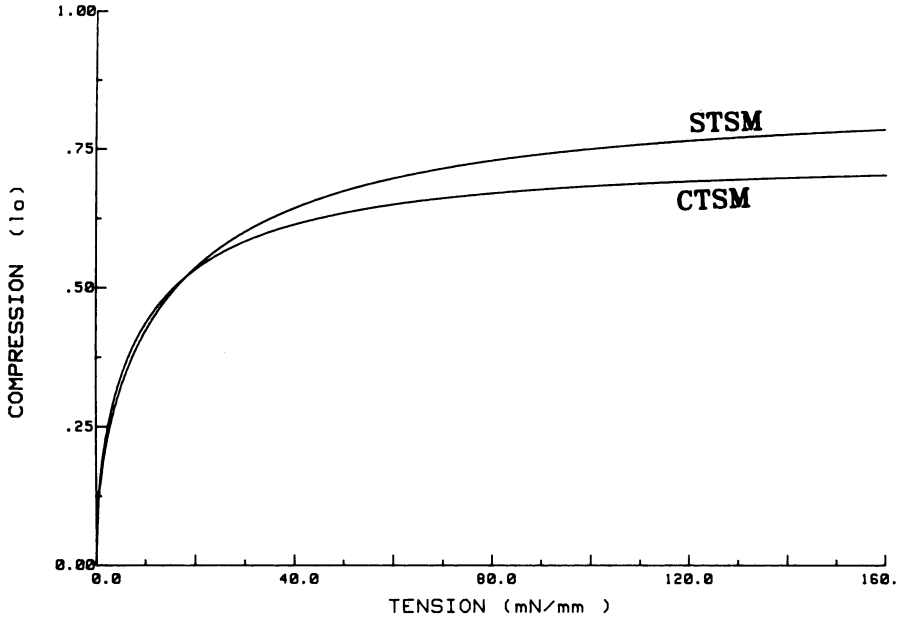

Fig. 15. Tension–compression curves for sensitized and control canine trachealis.

In smooth muscle a number of cytoskeletal proteins exist such as α-actinin, vinculin, desmin, vimentin, synaemin, filamin, plectin, four low-molecular-weight (18–30 kDa) cytosolic proteins (Rasmussen et al. 1987) and a separate 23 kDa protein. These could contribute to the IR. In this connection, Berner et al. (1981) have shown that in hypertensive VSM the earliest change that occurs is a remarkable increase in cytoskeletal proteins.

Biochemistry and Molecular Biology of Airway Smooth Muscle

This section is limited to consideration of the biochemistry of contractile and regulatory proteins of smooth muscle because this is most relevant to the mechanics of smooth muscle contraction. The energetics of contraction, of course, are just as relevant to contraction, but will not be dealt with here. Such studies of oxidative phosphorylation that we have conducted are reported and reviewed in the literature (Stephens and Wrogemann, 1970; Kroeger and Stephens, 1971; Stephens and Skoog, 1974; Stephens and Vogel, 1974).

Contractile Proteins

Myosin. The major protein of interest in smooth muscle, and on which most research has been conducted, is myosin. Although it structurally resembles that of skeletal muscle in that the molecule possesses two globular heads and a rodlike

tail with a high helical content and coiled-coil configuration, there are significant differences in enzyme activity. The myosin heads that can be enzymatically broken down into two subfragments (SF1 and SF2) contain distinct sites for binding to actin, ATP hydrolysis, and association of light chain subunits. The molecular weight of the molecule is approximately 470 kDa. Yanagisawa et al. (1987) have reported 1790 amino acid residues in the myosin heavy chain (MHC) polypeptide, which shows a calculated molecular weight of 228.9 kDa. The rod contains 1130 residues, of which 1090 contain no proline. The latter, therefore, form an uninterrupted α-helix. The remaining 40 residues form the irregular tail of the carboxyl terminal of the myosin heavy chain.

The myosin molecule consists of two heavy chains. Associated with these there are two sets of light chains; one is 17 kDa, about which little is known, and the other is 20 kDa (MLC20). The latter is the major regulatory protein in smooth muscles, in general, as well as in nonmuscle contractile systems.

Several isoforms of smooth muscle (SM) myosin heavy chain have been discovered. Those seen in the adult muscle consist of SM1 which has a molecular weight of 204 kDa and SM2 whose molecular weight is 200 kDa. The motility assay (Umemoto and Sellers, 1990) suggests the ATPase activity of these is the same. A third distinct form has been reported in the human pulmonary artery (Sartore et al., 1989). Two other isoforms have also been founded in mature smooth muscle. These were originally found in platelets and were therefore call nonmuscle myosin heavy chain (NMMHC). They have been found in practically all smooth muscles. Two NMMHC isoforms have been found of molecular weight 198 kDa and 196 kDa, respectively. Their ATPase activities have not yet been determined.

The two smooth muscle isoforms are distinguished by amino acid differences in their carboxy terminals. The difference is the result of alternative splicing of a single gene. A third, and likely important, isoform has been reported (Takahashi et al., 1993). It consists of an extra seven amino acid insert in the NH_2 terminal end that both ATP hydrolysis and actin binding occur. Furthermore, its ATPase activity (as judged from the motility assay) is almost three times greater than that of the other SM isoforms.

Smooth muscle does not possess any troponin system; rather, it is phosphorylation of MLC20 that is Ca^{2+} sensitive and regulates cross-bridge cycling, Tropomyosin (70 kDa) is present and consists of two subunits each of 35 kDa. As in skeletal muscle, tropomyosin is fibrous and lies in the groove between the two actin chains. Its role is not firmly established in smooth muscle, but it is likely similar to that in skeletal muscle. In *in vitro* experiments Chacko (1981) has reported that it modulates actin-activated myosin magnesium (Mg^{2+})-ATPase activity. The thick filament in smooth muscle is made up of several myosin molecules (number not established) and shows crossbridges or heads projecting from the rodlike thick filament. While the thick filament is 1.65 μm long in striated muscle, it is 2 μm long in smooth (Somlyo, 1980). It presumably carries more cross-bridges per half-sarcomere, which could be one reason why smooth muscle can develop as much stress as skeletal muscle in spite of possessing only one fifth the amount of myosin. Unlike skeletal muscle, it has been reported that

smooth muscle does not manifest a central bare area. The arrangement of myosin heads is not bipolar as in skeletal muscle, but side-polar.

Thick filaments are not normally seen in light and electron micrographs of smooth muscle, which is why it is termed *smooth*. Myosin, however, can be isolated quite easily from these muscles. This lack of filaments in light and electron micrographs has been shown to be artifactual. The filaments evidently disintegrate during section preparation. With the appropriate techniques, Somlyo et al. (1987) have shown that thick filaments are present both in resting and rigor (arrowhead) states. Thick filaments are evident, their orientation, which is parallel to the thin actin filaments, is also clearly seen. Furthermore, cross-bridges can be seen reaching out from the thick filament toward the thin. This provides the structural underpinning for believing the sliding filament, cross-bridge rotation theory of contraction also operates in smooth muscle contraction.

The ATPase activity of smooth muscle actomyosin is about 50 times lower than that of skeletal; however, there are a number of experimental factors (e.g., differences in temperature, pH, and osmolarity) that could account for the difference. The native molecule is a highly asymmetric hexamer. Under the electron microscope myosin molecules from vertebrate smooth muscle resemble those from both striated muscles and nonmuscle contractile systems. The tail of the smooth muscle myosin is 150 $\pm$ 20 nm in length. The amino acid sequence of smooth and skeletal myosins are the same; however, there are differences in arginine, leucine, glycine, valine, and isoleucine contents (Frederiksen, 1979). The α-helical conformation in aortic myosin contains 200–400 amino acids more than in skeletal; this may contribute to immunologic differences between the two (Groschel-Stewart, 1982).

Although the skeletal muscle myosin molecule has two hinge regions, it appears that the smooth muscle myosin contains only one. This is situated a little distance away from the junction of the head and the tail (Cross, 1988); however, others report two hinge regions in the tail (Onishi, 1982). It is likely the second is revealed when binding of the tail in 10S configuration (Cross, 1988) occurs.

Proteolytic subfragments can be obtained from the smooth muscle myosin molecule. The rodlike light meromyosin (LMM) fragment obtained by treatment with chymotrypsin is longer than that from the skeletal myosin molecule. In chicken gizzard myosin the combined LMM and SF2 constitute the myosin rod which is 156 nm in length.

The rod obtained from pig stomach myosin can be further digested to yield a 13 kDa segment from the carboxyl terminal. Its importance is in enabling myosin molecule assembly (Cross, 1986).

Digestion of SFI (perhaps the most functionally important part of the molecule) of the smooth muscle heavy meromyosin, yields an amino terminal 25 kDa fragment, a central 50 kDa fragment, and a 20 kDa carboxy terminal fragment (Marianne-Pepin et al., 1983). The linkage between the two latter fragments undergoes the conformational change that is operative in the 10 to 6S transition. The central 500 Da fragment is the site for nucleotide binding (Bonet et al., 1987). The carboxyl terminal end of the fragment is the site for the binding of myosin light chain (MLC).

With respect to genetic control, evidence for two MHC-messenger ribonucleic acids (mRNAs) has been deduced from nuclease S1 protection experiments (Ngai and Walsh, 1987) in smooth muscle. Gene transcription and translation has not yet been studied in smooth muscle.

As mentioned earlier, two (MLC) are present in the myosin molecule. The 17 kDa molecule, whose function is not yet known, is present in two isoforms in uterine smooth muscle. Cavaille et al. (1986) report their stoichiometry varies during pregnancy and may influence actomyosin ATPase activity, even though myosin heavy chain isozyme distribution patterns do not vary.

There are four isoforms of the 20 kDa MLC in the uterus (Barany et al., 1987). In VSM Erdodi et al. (1987) have reported two isoforms. The nonphosphorylated (MLC20) appears as two bands on two-dimensional gel electrophoresis. Their ratio is 85:15. Phosphorylation of MLC20 will be discussed after dealing with actin. It appears that both muscle and nonmuscular isoforms of MLC20 are present. Isoforms of the 17 kDA myosin light chain (MLC17) have also been reported; one is acidic MLCa, the other alkaline MLC17b. It is somewhat surprising that V_o is more closely related to MLC17 activity than to myosin heavy chains.

An embryonic form of MLC has also been reported. Its molecular weight is 23 kDA and it appears only transiently.

Actin

Actin is a major contractile and structural protein in smooth muscle. With respect to the latter, nonmuscle actin isoforms may be used predominantly for cytoskeletal functions.

ASM actin has not yet been studied, but because the molecule is very highly conserved in nature it is likely to be very similar to that of skeletal.

Turkey gizzard myofibril protein, whose actin consists of 75% smooth muscle γ-isoactin and 25% nonmuscle β-isoactin, can be separated into an actomyosin and a cytoskeletal fraction. The major actin in a muscle is the major form involved in force generation.

At least eight isoactins have been identified in mammalian cells whose pattern of distribution is tissue specific (Rupinstem, 1990). Skeletal and cardiac muscle contain only α-actin; nonmuscle cells contain β- and γ-actin. The functional significance of multiple actins in avian, and mammalian cells is not known.

On the basis of mobility on isoelectric focusing gels, the actins have been termed α, β, and γ in order of increasing basicity. There are also several isoactins that characterize different muscles. For example, α-skeletal and α-cardiac, and both an α- and a γ-smooth muscle actin are known to be present. The predominant VSM isoactin is the α-isoform, whereas it is γ in intestinal smooth muscle. A characteristic feature of smooth muscle is that 50% the actin is of the nonmuscle type.

In smooth muscle, as in all muscle cells, the chief action of actin is to activate the Mg^{2+}-ATPase activity of myosin. This actin activation is made possible by the phosphorylation of MLC20 (Sobieszek, 1977; deLanerolle et al., 1982) in smooth muscle. The phosphorylation is induced by MLC kinase, whose catalytic

subunit is activated by the binding of the 4S Ca^{2+}-calmodulin complex to it. The extent of phosphorylation of MLC20 increases from 0.04 to 0.8 mol/Pi/mol MLC20 with a pseudo–first-order rate of 1.1/second; this was reported by Kamm and Stull (1985) for bovine TSM. Using a method developed for detecting diphosphorylation of MLC20, they reported that the extent of phosphorylation in "nonphosphorylated," monophosphorylated, and diphosphorylated myosin was 0.2, 0.6, and 1 mol Pi/mol light chain.

Myosin Light Chain Kinase in Airway Smooth Muscle

The various domains of this molecule have now been determined, chiefly with the help of proteolytic enzymes. When isolated from turkey gizzard, myosin light chain kinase (MLCK) was found to be a 140 kDa molecule. The domains identified are the catalytic or constitutive, the calmodulin-binding and the cAMP-dependent protein kinase phosphorylatable (Foyt et al., 1985). Ito et al. (1991) have also identified that a critical region of the inhibitory domain is contained within the sequence Tyr-794-Trp-800 that overlaps with the calmodulin-binding site for five residues. This localization of an inhibitory sequence is consistent with autoinhibition via a pseudosubstrate domain. In summary the domains are a substrate-binding domain that is adjacent to the catalytic domain, followed by a regulatory domain that contains the calmodulin binding domain and the pseudosubstrate domain. It has been shown that calmodulin is the major binding site for Ca^{2+} in smooth muscle. Its structure reveals an eight-turn helix that separates the two pairs of Ca^{2+} binding sites. It is this region that is important for enzyme recognition and activation. The amino-terminal region of the sequence of the calmodulin-binding region of the smooth muscle MLCK serves to inhibit the enzyme from binding substrate in the absence of calmodulin (i.e., it is a pseudosubstrate region). From a therapeutic point of view it is speculated that inhibitors directed toward this intermolecular reaction should provide new drugs for the treatment of asthma and essential hypertension.

Sobieszek (1991) has deduced from kinetic data that MLCK could exist in several oligomeric forms, with an inactive high molecular size form and an active low molecular size form. Our own studies of this important enzyme will be discussed later in the section on changes in sensitized ASM. Gallagher (personal communication) has reported that adult (MW 140 kDa) and embryonic or nonmuscular forms are present. The molecular weight of the latter is 205 kDa. A third form, recently report is the endothelial cell type whose molecular weight is 214 kDa. It exists in soluble cytosolic and insoluble cytoskeletal forms. Its function is unknown. We have found this form in canine ASM.

Caldesmon

This relatively recently discovered molecule has kindled considerable interest because it provides an alternate mechanism for the regulation of smooth muscle contraction: thin-filament linked regulation.

Caldesmon was first isolated and named by Sobue et al. (1981) on the basis of its Ca^{2+}-dependent interaction with calmodulin. It occurs in two sizes of species, 135 and 140 kDa. There are several isoelectric variants in the chicken gizzard, and though its amino acid sequence structure has not been published, a cyclic deoxyribonucleic acid (CDNA) probe has been cloned by Imai et al. (1989).

The interaction with calmodulin is Ca^{2+}-dependent, whereas the actin interaction is independent of the free Ca^{2+} concentration. *In situ* caldesmon is bound to the actin filament.

With respect to function, the inhibition of actomyosin ATPase activity by a so-called flip-flop mechanism, does not seem tenable as the concentration of Ca^{2+}-calmodulin required is very high (Sobue et al., 1982). Notwithstanding that, Ngai and Walsh (1987) have suggested that the inhibitory effect of caldesmon on actomyosin ATPase may be blocked by reversible phosphorylation of the former. The kinase and phosphatase involved have been isolated. These authors have suggested that caldesmon may be involved in the regulation of the latchbridge and conclude that the former is always bound to the thin filament, but its interaction with myosin is regulated by phosphorylation.

Calponin

Takahashi et al. (1986) have isolated another peptide called *calponin* and suggested that it may also regulate contraction in smooth muscle. It inhibits the actin-activated Mg^{2+} ATPase activity of smooth muscle myosin, but without affecting MLC20 phosphorylation. Winder and Walsh (1990) showed that Ca^{2+}-dependent phosphorylation of calponin resulted in loss of its ability to inhibit the actomyosin ATPase, and reduction in actin binding.

Calponin has also been isolated from bovine aorta. It is a heat-stable, basic, 34 kDa protein which, as suggested, interacts with F-actin and tropomyosin in a Ca^{2+}-independent manner and with calmodulin in a Ca^{2+}-dependent manner. It is present in smooth muscle at the same molar concentration as tropomyosin, is a thin filament protein and binds to tropomyosin with a binding pattern similar to that of skeletal muscle troponin T.

Conclusions

The tempo of research on ASM has picked up considerably since 1990 particularly because of the importance of elucidating the pathogenesis of asthma (see chapter 22 by Barnes). The research attack has shifted to study of the cell biology and pathobiology of airway smooth muscle cells. We are also seeing the onset of application of methods of molecular genetics and molecular biology to the problems of asthma. Research of the airway smooth muscle itself lags behind that devoted to the role of chronic inflammation in asthma. Our own studies indicate that the cause of increased asthmatic bronchoconstriction is increased myosin light chain kinase activity. This is the result of increased kinase content; specific

activity is unchanged (Stephens, Li, Wang, and Ma, 1998). Future studies will need to focus on the cause of the increased MLC and content.

References

Abe Y, Tomita T (1968) Cable properties of smooth muscle. J Physiol (Lond) 196:87–100

Akasaka K, Konno K, Ono Y, Mue S, Abe C (1975) Electromyographic study of bronchial smooth muscle in bronchial asthma. Tohoki J Exp Med 117(1):55–59

Aksoy MO, Murphy RA, Kamm KE (1982) Role of Ca^{++} and myosin light chain phosphorylation in regulation of smooth muscle. Am J Physiol 242:109

Antonissen LA, Mitchell RW, Kepron W, Tse TS, Stephens NL (1979) Mechanical alterations of airway smooth muscle in a canine asthmatic model. J Appl Physiol 46:681

Baba K, Baron CB, Coburn RF (1988) Phorbol ester-induced conanical coupling in the response of swine tracheal smooth muscle to carbachol. FASEB J 2:A33

Bagby RM, Young AM, Dotson RS, Fisher BA, McKinnon K (1971) Contraction of single smooth muscle cells from Bufo marinus stomach. Nature 234:351–352

Barany K, Csabina S, deLanerolle P, Barany M (1987) Evidence for isoforms of the phosphorylatable myosin light chain in rat uterus. Biochim Biophys Acta 911:369–371

Baron CB, Coburn RF (1987) Inositol phospholipid turnover during contraction of canine trachealis muscle. Ann NY Acad Sci 494:80–83

Baron CF (1989) Transduction and signalling in airway smooth muscle. In: Coburn RF (ed) Airway Smooth Muscle in Health and Disease. Plenum, New York, pp 127–149

Bean BP, Sturck M, Puga A, Henmsmeyer K (1986) Calcium channels in muscle cells isolated from rat mesenteric arteries: modulation by kihydropyridine drugs. Circ Res 59:229–235

Berner BP, Somlyo AV, Somlyo AP (1981) Hypertrophy-induced increase of intermediate filaments in vascular smooth muscle. J Cell Biol 88:96–101

Bonet A, Mornet D, Audemard E, Deraucourt J, Bertrand R, Kassab R (1987) Comparative structure of the protease-sensitive regions of the subfragment-I heavy chain from smooth and skeletal muscle myosin. J Biol Chem 262:16524–16530

Brutsaert DL, Claes VA, Sonnenblick EH. Effects of abrupt load alterations on force-velocity length and time relations during isotonic contractions of heart muscle: load clamping. J Physiol (Lond) 216:319

Burnstock G (1979) Structure of smooth muscle and its innervation. In: Brading A, Jones AE, Tomita T (eds) Smooth Muscle. Arnold, London, pp 1–69

Butler TM, Siegman MJ, Mooers SU (1983) Chemical energy usage during shortening and work production in mammalian smooth muscle. Am J Physiol 244:C234

Cavaille E, Jannot C, Ropert S, d'Albis A (1986) Isoforms of myosin and actin in humans, monkey and rat myometrium comparison of pregnant and non-pregnant uterus proteins. Eur J Biochem 160:507–513

Chacko S (1981) Effects of phosphorylation, calcium ion, and tropomyosin on actin-actiated adenosine 5′-triphosphatase activity of mammalian smooth muscle myosin. Biochem J 20:702–707

Coburn RF, Tomita T (1973) Evidence for nonadrenergic inhibitory nerves in the guinea pig trachealis muscle. Am J Physiol 224:1072–1080

Coburn RF, Yamaguchi T (1977) Membrane potential-dependent and -independent tension in the canine tracheal mucle. J Pharmacol Exp Ther 201:276–284

Cross RA (1988) Smooth muscle contraction. What is 10s myosin for? J Musc Res Cell Motil 9:108–110

Cross RA, Vandekerckhove J (1986) Solubility-determining domain of smooth muscle myosin rod. FEBS Lett 200:355–360

Dahlstrom AK, Fune T, Hokfelt T, Norbet K (1966) Adrenergic innervation of the bronchial muscle of the cat. Acta Physiol Scand 66:507–508

Daniel EE, Kannan M, Davis C, Posey-Daniel V (1986) Ultrastructural studies on the neuromuscular control of human tracheal and bronchial muscle. Res Physiol 63:109–128

deLanerolle R, Condit JR, Tanenbaum M, Adelstein RS (1982) Myosin phosphorylation, agonist concentration, and contraction of tracheal smooth muscle. Nature 298:871–872

Dillon PF, Aksoy MO, Driska SP, Murphy RA (1981) Myosin phosphorylation and the crossbridge cycle in arterial smooth muscle. Science 211:495–497

El-Bermani AW, McNary F, Bradley DS (1970) The distribution of acetylcholinesterase and catecholamine containing nerves in the rat lung. Anat Rec 167:207–212

Erdodi F, Barany M, Barany K (1987) Myosin light chain isoforms and their phosphorylation in arterial smooth muscle. Circ Res 61:898–903

Fay FS (1977) Mechanics of single isolated smooth muscle cells. In: Casteels R, Godfraind T, Ruegg JC (eds) Excitation Contraction Coupling in Smooth Muscle. Elsevier/North Holland, Amsterdam, pp 433–439

Fay FS, Fogarty K, Fujiwara K (1984) The organization of the contractile apparatus in single isolated smooth muscle cells. In: Stephens NL (ed) Smooth Muscle Contraction. Marcel Dekker, New York, pp 75–89

Foyt HL, Guerriero V, Means AR (1985) Functional domains of chicken gizzard myosin light chain kinase. J Biol Chem 260:7765–7774

Frederiksen DW (1979) Physical properties of myosin from aortic smooth muscle. Biochem J 18:1651–1656

Fung YC (1981) The meaning of the constitutive equation. In: Biomechanics, Mechanical Properties of Living Tissue. Springer-Verlag, New York, pp 22–61

Gabella G (1976) Structural changes in smooth muscle cells during isotonic contraction. Cell Tissue Res 170:187–201

Gorecka A, Aksoy MO, Hartshorne DJ (1974) The effect of phosphorylation of gizzard myosin on actin activation. Biochem Biophys Res Commun 71:325

Groschel-Stewart U, Drenkhahtor D (1982) Muscular and cytoplasmic contractile proteins. Collagen Res 2:381–463

Groschel-Stewart U, Chamley JH, McConnell JR, Brunstock G (1975) Comparison of the reaction of cultured smooth and cardiac muscle cells and fibroblasts to specific antibodies to myosin. Histochemistry 43:215–225

Hakansson CH, Mercke U, Sonesson B, Toremalon NG (1976) Functional anatomy of the musculature of the trachea. Acta Morphol Neer I Scand 14(4):291–297

Hargreave FE, et al (1980) Allergen-induced airway responses and relationships with nonspecific airway reactivity. In: Hargreave FE (ed) Airway Reactivity. Astra, Mississauga, ON, pp 145–150

Hellstrand P, Johansson B (1979) Analysis of the length response to a free step in smooth muscle. Acta Physiol Scand 106:221–238

Hill AV (1938–1939) The heat of shortening and the dynamic constants of muscle. Proc R Soc Lond Biol 126:136

Imai M, Dunn L, Lee R, Cook R, May G, Bryan J (1989) Molecular cloning of caldesmon cDNA. J Cell Biol 107:A681

Irwin CG, Bioleau R, Tremblay J, Martin RR, Macklem PT (1980) Bronchodilatation: non-cholinergic, nonadrenergic mediation demonstrated in vivo in the cat. Science 207:791–792

Ito M, Guerriero V, Chen X, Hartshorne DJ (1991) Definition of the inhibitory domain of smooth muscle myosin light chain kinase by site-directed mutagenesis. Biochem J 30:3498–3503

Jenne J, et al (1975) Induction of β-receptor tolerance by terbutaline. J Allergy Clin Immunol 55:96

Jewell BR (1974) Discussion of S.R. Taylor, Decreased activation in skeletal muscle fibers at short lengths. In: Porter R, Fitzsimons DW (eds) The Physiological Basis of Startling's Law of the Heart. Ciba Symposium 24. Elsevier/Excerpta, Medica/North Holland, Amsterdam, pp 93–116

Johansson B (1978) Mechanics of smooth muscle relaxation. In: Vanhoutte PM, Levsen IS, Karger AG (eds) Mechanisms of Vasodilatation. S. Karger, Basel, pp 48–55

Kamm KE, Stull JT (1985) Myosin phosphorylation, force, and maximal shortening velocity in neurally stimulated tracheal smooth muscle. Am J Physiol 249:C238–C247

Kirkpatrick CT (1975) Excitation and contraction in bovine tracheal smooth muscle. J Physiol (Lond) 44:263–281

Klöckner U, Isenberg G (1985) Calcium activated potassium currents as an indicator for intracellular Ca^{2+} transients (single smooth muscle cells from trachea and urinary bladder). Pflugers Arch 405:R61

Kotlikoff MR (1989) Ion channels in airway smooth muscle. In: Airway Smooth Muscle in Health and Disease. Plenum Press, New York, pp 169–182

Kotlikoff MI (1988) Calcium currents in isolated canine airway smooth muscle cells. Am J Physiol 254:C793–C808

Kroeger EA, Stephens NL (1975) Effect of tetraethylammonium ion on airway smooth muscle: imitation of phasic electrical activity. Am J Physiol 228:633–636

Kroeger EA, Stephens NL (1971) Effect of hypoxia on energy and calcium metabolism in airway smooth muscle. Am J Physiol 220:1199

Marianne-Pepin T, Mornet D, Audemard E, Kassab R (1983) Structural and actin-binding properties of the trypsin produced HMM and S-1 from gizzard smooth muscle myosin. FEBS Lett 159:211–216

Mitra R, Morad M (1985) Ca^{2+} and Ca^{2+}-activated K^{+} currents in mammalian gastric smooth muscle cells. Science 229:269–272

Moreno RH, Hogg JC, Pare PD (1980) Mechanics of airway narrowing. Am Rev Respir Dis 133:1171

Mrwa U, Ruegg JC (1975) Myosin-linked calcium regulation in vascular smooth muscle. FEBS Lett 60–81

Mulvaney MJ (1979) The undamped and damped series elastic components of a vascular smooth muscle. Biophys J 26:401

Ngai PK, Walsh MP (1987) The effects of phosphorylation of smooth muscle caldesmon. Biochem J 244:417–425

O'Donnel SR, Sarr N (1973) Histochemical localization of adrenergic nerves in the guinea pig trachea. Br J Pharmacol 47:707–710

Ohya Y, Kitanura K, Kuriyama H (1988) Regulation of calcium current by intracellular calcium in smooth muscle cells of rabbit portal vein. Circ Res 62:375–383

Onishi H, Wakabayashi T (1982) Electronmicroscopic studies of myosin molecules from chicken gizzard I: the formation of the intramolecular loop in the myosin tail. J Biochem (Tokyo) 92:871–879

Paul RJ, Gluck E, Ruegg JC (1976) Crossbridge ATP utilization in arterial smooth muscle. Pflugers Arch: Eur J Physiol 361:297–299

Peterson JW, Evans RJC, Prime FJ (1971) Selectivity of bronchodilator action of salbutamol in asthmatic patients. Br J Dis Chest 65:22

Rasmussen H, Takuwd Y, Park S (1987) Protein kinase C in the regulation of smooth muscle contraction. FASEB J 1:177–185

Richardson JB, Ferguson CC (1979) Neuromuscular structure and function in the airways. Fed Proc 38(2):202–208

Richardson JB, Bouchard T (1975) Demonstration of a nonadrenergic inhibitory nervous system in the trachea of the guinea pig. J Allergy Clin Immunol 56:473–480

Richardson JB, Beland J (1976) Nonadrenergic inhibitory nerves in human airways. J Appl Physiol 41:764–771

Roach MR, Burton AC (1957) The reason for the shape of the distensibility curves of arteries. Can J Biochem Physiol 35:681

Rubinstein PA (1990) The functional importance of multiple actin isoforms. Bioessays 12:309–315

Rudel R, Taylor SR (1971) Striated muscle fibers: facilitation of contraction at short lengths by carreine. Science 172:387

Russell JA (1978) Responses of isolated canine airways to electric stimulation and acetycholine. J Appl Physiol 45:690

Sartore S, DeMarzo N, Barrione A-C, Zanellato AMC, Saggin L, Fabbri L, Schiaffino S, et al (1989) Myosin heavy chain isoforms in human smooth muscle. Eur J Biochem 179:79–85

Schmid A, Barhanin J, Coppola T, Borsotto M, Lazdionski M (1986) Immunochemical analysis of subunit structures of dependent Ca^{2+} channels in skeletal, cardiac, and smooth muscles. Biochem 25:3492–3495

Seow CY, Stephens NL (1989) Changes of tracheal smooth muscle stiffness during an isotonic contraction. Am J Physiol 256:C341–C350

Seow C, Stephens NL (1987) Time dependence of series elasticity in tracheal smooth muscle. J Appl Physiol 62(4):1556–1561

Sobieszek A (1977) Vertebrate smooth muscle myosin. Enzymatic and structural properties. In: Stephens NL (ed) The Biochemistry of Smooth Muscle. University Park Press, Baltimore, pp 413– 443

Sobieszek A (1991) Regulation of smooth muscle myosin light chain kinase. J Mol Biol 220:947–957

Sobue K, Morimoto K, Inui M, Kanda K, Kakiuchi S (1982) Control of actin-myosin interaction of gizzard smooth muscle by calmodulin- and caldesmon-linked flip-flop mechanism. Biomed Res 3:188–196

Sobue K, Muramoto Y, Fujita M, Kakiuchi S (1981) Purification of a calmodulin-binding protein from chicken gizzard that interacts with F-actin. Proc Natl Acad Sci USA 78:5652–5655

Somlyo AV, Goldman Y, Fujimori T, Bond M, Trentham D, Somlyo AP (1987) Crossbridge transients initiated by photolysis of caged nucleotides and crossbridge structure in smooth muscle. In: Siegman MJ, Somlyo AP, Stephens NL (eds) Regulation and contraction of smooth muscle. Alan Liss, New York, pp 27–41

Somlyo AV (1980) Ultrastructure of vascular smooth muscle. In: Bohr DF, Somlyo AD, Sparks HV (eds) Handbook of Physiology—Vascular Smooth Muscle. Williams and Wilkins, Baltimore pp 310–324

Somlyo AV (1980) Ultrastructure of vascular smooth muscle. In: Bohr DF, Somlyo AD, Sparks HV (eds) Handbook of Physiology Section 2: The Cardiovascular System. American Physiological Society, Bethesda, pp 33–68

Somlyo AV, Somlyo AP (1968) Electromechanical and pharmacomechanical coupling in vascular smooth muscle. J Pharmacol Exp Ther 159:129–145

Souhrada JF, Dickey DC (1976) Effect of antigen challenge on sensitized guinea pig trachea. Respir Physiol 27:241

Souhrada JR, Loader J (1979) Changes of airway smooth muscle in experimental asthma. In: deKock MA, Nadel JA, Lewis CM (eds) Mechanisms of Airways Obstruction in Human Respiratory Disease. AA Balkema, Capetown, pp 195–207

Stephens NL, Kromer U (1971) Series elastic component of tracheal smooth muscle. Am J Physiol 220:1890–1895

Stephens NL, Kroeger EA (1980) Ultrastructure, biophysics, and biochemistry of airway smooth muscle. In: Nadel JA (ed) Physiology and Pharmacology of the Airways. Marcel Dekker, New York, pp 31–42

Stephens NL, Kagan ML, Packer CS (1980) Time dependence of shortening velocity in tracheal smooth muscle. Am J Physiol 251:C435

Stephens NL, Van Niekerk W (1977) Isometric and isotonic contractions in airway smooth muscle. Can J Physiol Pharmacol 55:933

Stephens NL, Vogel J (1974) Oxidative phosphorylation in hypoxic airway smooth muscle. Can J Physiol Pharmacol 52:84–89

Stephens NL, Skoog CA (1974) Tracheal smooth muscle and rate of oxygen uptake. Am J Physiol 226:1462–1467

Stephens NL (1972) Mechanism of action of hypoxia in tracheal smooth muscle (TSM) with a note on the role of the series elastic component. In: Betz E (ed) Vascular Smooth Muscle. Springer-Verlag, Berlin, pp 153–156

Stephens NL (1975) Physical properties of contractile systems. In: Daniel EE, Paton EE (eds) Methods in Pharmacology, Vol 3. Smooth Muscle. Plenum, New York, pp 165–196

Stephens NL, Mitchell R, Brutsaert DL (1983) Nature of contractile unit: shortening inactivation. Maximum force potential, relaxation, contractility. In: Stephens NL (ed) Smooth Muscle Contraction. Marcel Dekker, New York

Stephens NL, Vogel J (1972) Mechanism of actin of hypoxia in tracheal smooth muscle (TSM) with a note on the role of the series elastic component. In: Betz E (ed) Vascular Smooth Muscle. Springer-Verlag, Berlin, pp 153–156

Stephens NL (1970) The mechanics of isolated airway smooth muscle. In: Bouhuys A (ed) Airway Dynamics. Thomas, Springfield Il, pp 191–208

Stephens NL, Wrogemann K (1970) Oxidative phosphorylation in smooth muscle. Am J Physiol 219(6):1796–1801

Stephens NL, Hoppins EG Jr (1980) Mechanical properties of airway smooth muscle. In: Handbook of Physiology—The Respiratory System III. American Physiology, Washington DC, pp 264–276

Stephens NL, Kong SK, Seow CY (1988) Mechanism of increased shortening of sensitized airway smooth muscle. In: Armour CL, Black JL (eds) Mechanism in Asthma: Pharmacology, Physiology and Management. Alan Liss, New York, pp 231–254

Stephens NL (1977) Airway smooth muscle: biophysics, biochemistry, and pharmacology. In: Lichensteina dn LM, Austen KF (eds) Asthma: Physiology, Immunopharmacology, and Treatment. Academic Press, New York, pp 147–167

Suzuki H, Morita K, Kuriyama H (1976) Innervation and properties of the smooth muscle of the dog trachea. Jpn J Physiol 26:303–320

Takahashi K, Hiwada K, Kokobu T (1986) Isolation and characterization of a 2300-Dalton Calmodulin- and F-actin-binding protein from chicken gizzard smooth muscle. Biochem Biophys Res Comm 141:20–26

Takahashi M, Yu JH, Adelstein RS (1993) An insert of seven amino acids confers enzymatic differences between smooth muscle myosins from the intestines and vasculature. J Biol Chem 268:12848–12854

Taylor S (1974) Decreased activation in skeletal muscle fibers at short lengths. In: Porter R, Fitzsimons W (eds) The Physiological Basis of Startling Law of the Heart. Ciba Symp. Elsevier/Excerpta, Medical North Holland, Amsterdam, pp 93–116

ter Keurs HEDJ, Iwazumi T (1988) Resting forces in cardiac myocytes and ultrasmall trabeculae. Biophys J 53:167a

Umemoto S, Sellers JR (1990) Characterization of in vitro motility assays using smooth muscle and cytoplasmic myosins. J Biol Chem 265(25):14864–14869

Vanpeperstraete F (1973) The cartilaginous skeleton of the bronchial tree. Adv Anat Embryol Cell Biol 48(3):1–80

Wang Z, Stephens NL (1989) Normally cycling and latch bridge in venous smooth muscle. Blood Vessels 26(5):272–279

Wang Z, Seow CY, Stephens NL (1988) Mechanical properties of isolated canine coronary artery. FASEB J 2(4):A333

Winder SJ, Walsh MP (1990) Smooth muscle calponin. J Biol Chem 265:148–155

Woledge RC, Curtin NA, Homsher E (1985) Energetic aspects of muscle contraction. Academic Press, Orlando, pp 27–117

Xu J, et al (1980) Mechanical properties of inbred hyperactive rat trachealis. FASEB J 4(3):A269

Yanagisawa M, Handa Y, Kataswagawa Y, Imamura M, Mikawa T, Masaki T (1987) Complete primary structure of vertebrate smooth muscle myosin heavy chain deduced from its complementary DNA sequence. J Mol Biol 198:143–157

Accepted for publication: 10 January 2002